Single-particle Cryo-EM -- Visualization of Biological Molecules in their Native States

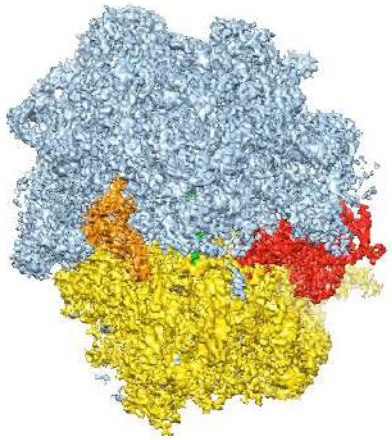

Joachim Frank
Department of Biochemistry and Molecular Biophysics
Department of Biological Sciences
Columbia University

Funding : National Institutes of Health

Molecular Machines in the Cell

ATP Synthase

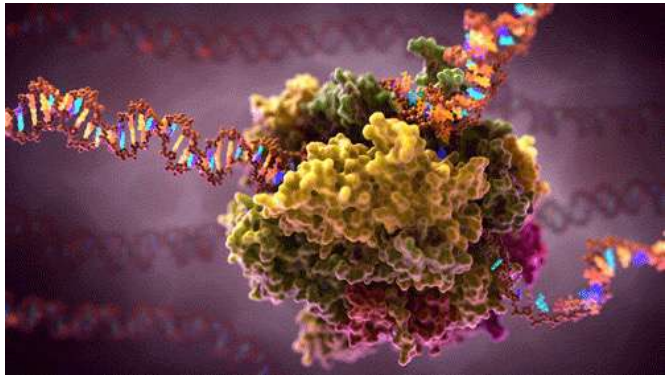

RNA Polymerase *(Art of the Cell)*

Bruce Alberts, Cell 1998

- Molecular machines: many molecules act in concert, in a processive way
- We wish to know the structures of all components but also the way they interact dynamically
- Reductionism: we study a subsystem in isolation (in vitro), hoping to approximate the processes in the environment of the cell
-

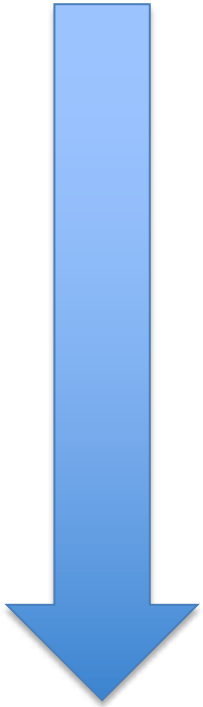

- Ancient history, EM and X-ray crystallography
- 1975 Single particle techniques -- the concept
- 1975 – 1987 SPIDER, programs for averaging, classification, 3D reconstruction
- 1981 Dubochet's discovery of vitreous ice
- 1987 First single-particle reconstruction – negative stain
- 1989 First single particle reconstruction – vitreous ice
- 1990 – 2012 Cryo-EM reconstructions with increasing resolutions up to 5.5 Angstrom
- 2012 Direct electron detection cameras hit the market
- 2012 – now "resolution revolution"
- TODAY: exponential increase in cryo-EM structure depositions
- Future: Time-resolved cryo-EM & Mapping of continuum of states using cryo-EM

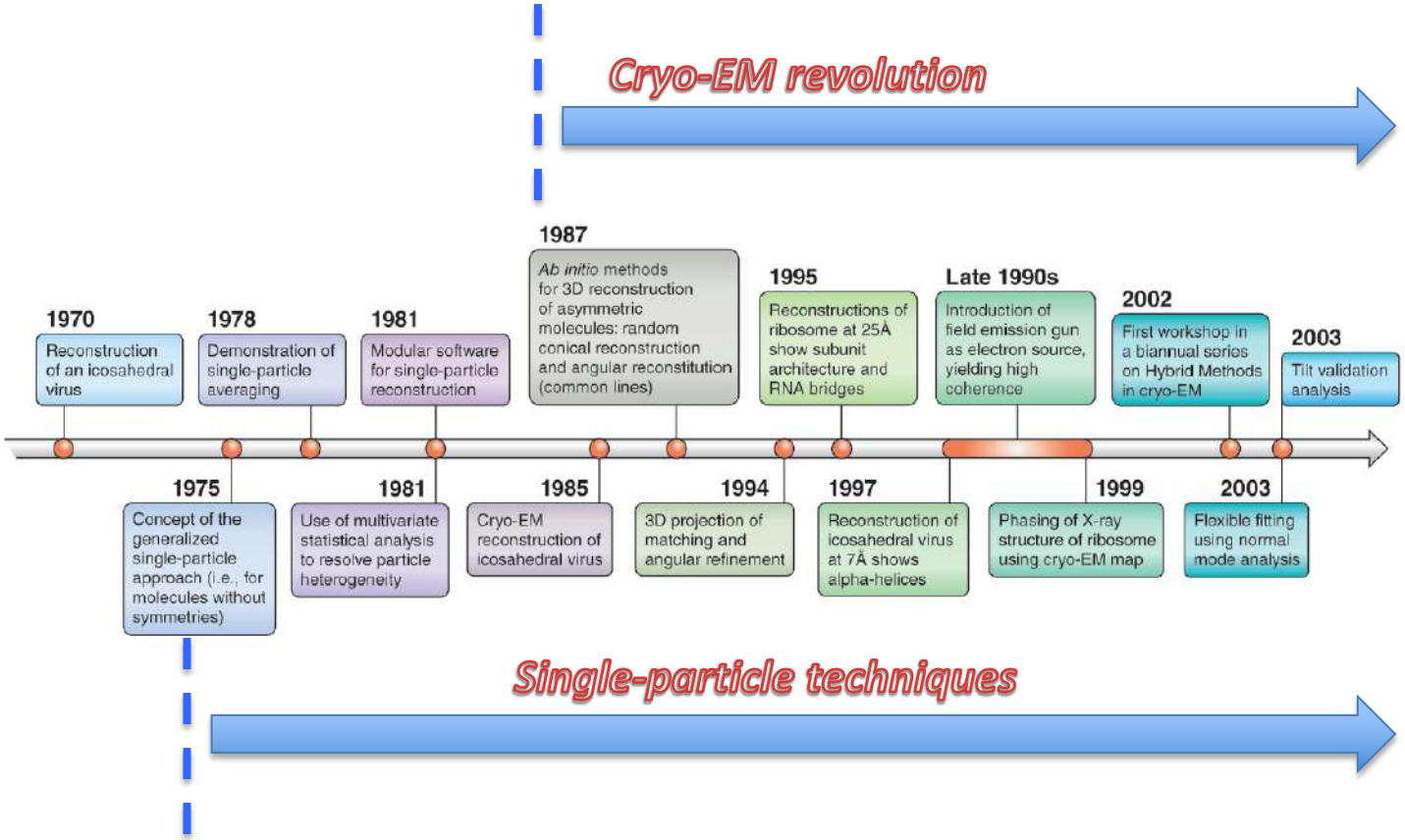

J. Frank, Nature Protocols 2017

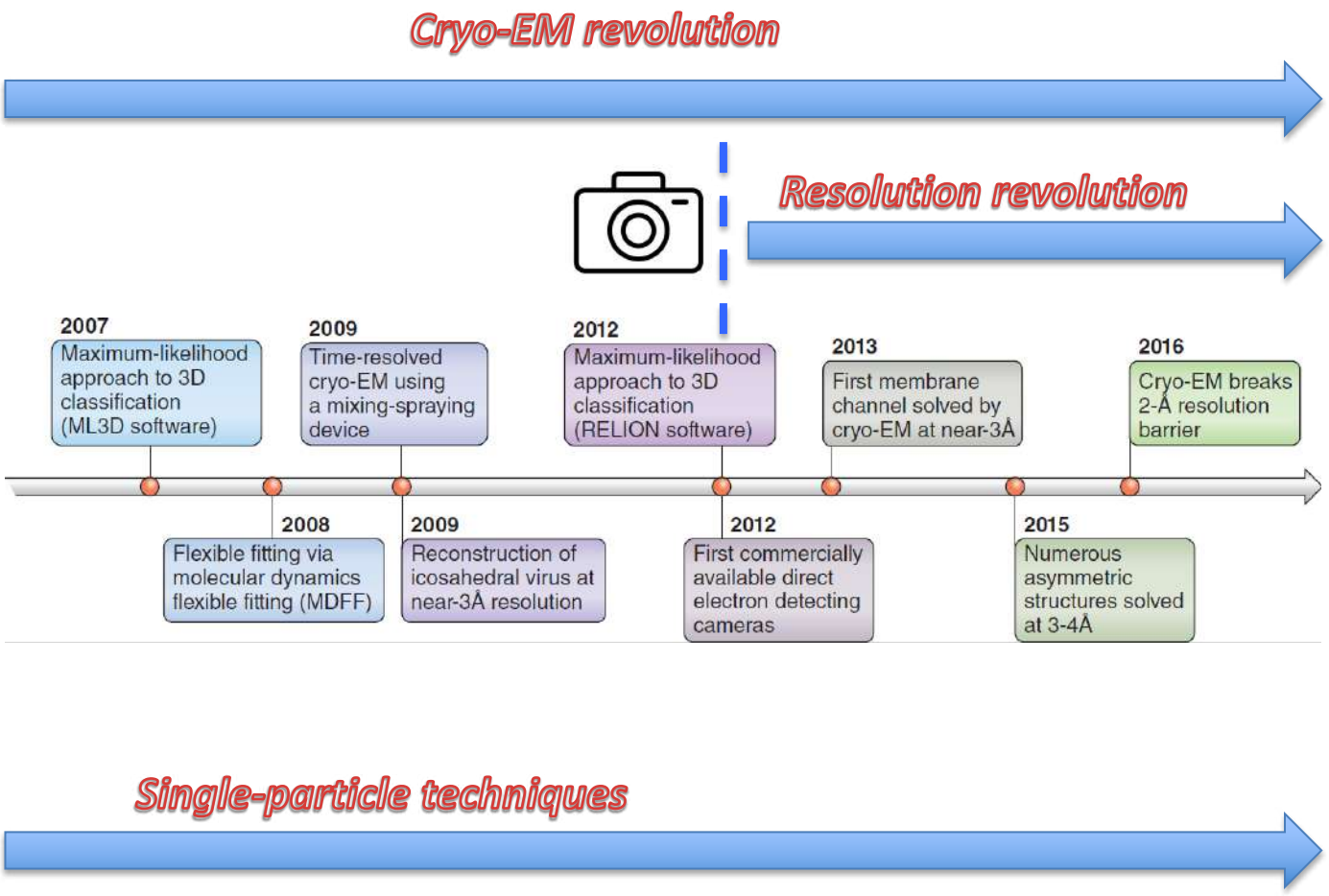

J. Frank, Nature Protocols 2017

X-ray Crystallography

- Crystal: many copies of the molecule arranged in regular order.
- *Exposure to X-ray beam → diffraction pattern → structure determination.*
- X-ray beam must be high-intensity, crystal must be almost perfect.
- *To date ~ 140,000 structures solved by X-ray crystallography, available in public databanks.*
- Crystal packing → molecules not visualized in all conformations/binding states that important for function.
- *Many molecules do not form highly ordered crystals.*
- Sample quantity can be a big issue, as well.
-

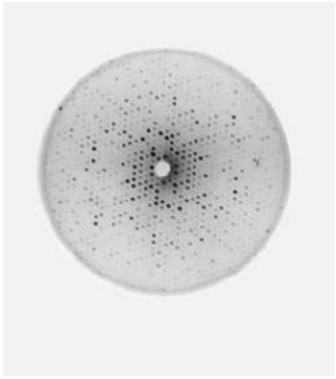

Max Perutz and John Kendrew with a model of hemoglobin, 1962

http://www.mfpl.ac.at/vips/max-f-perutz/

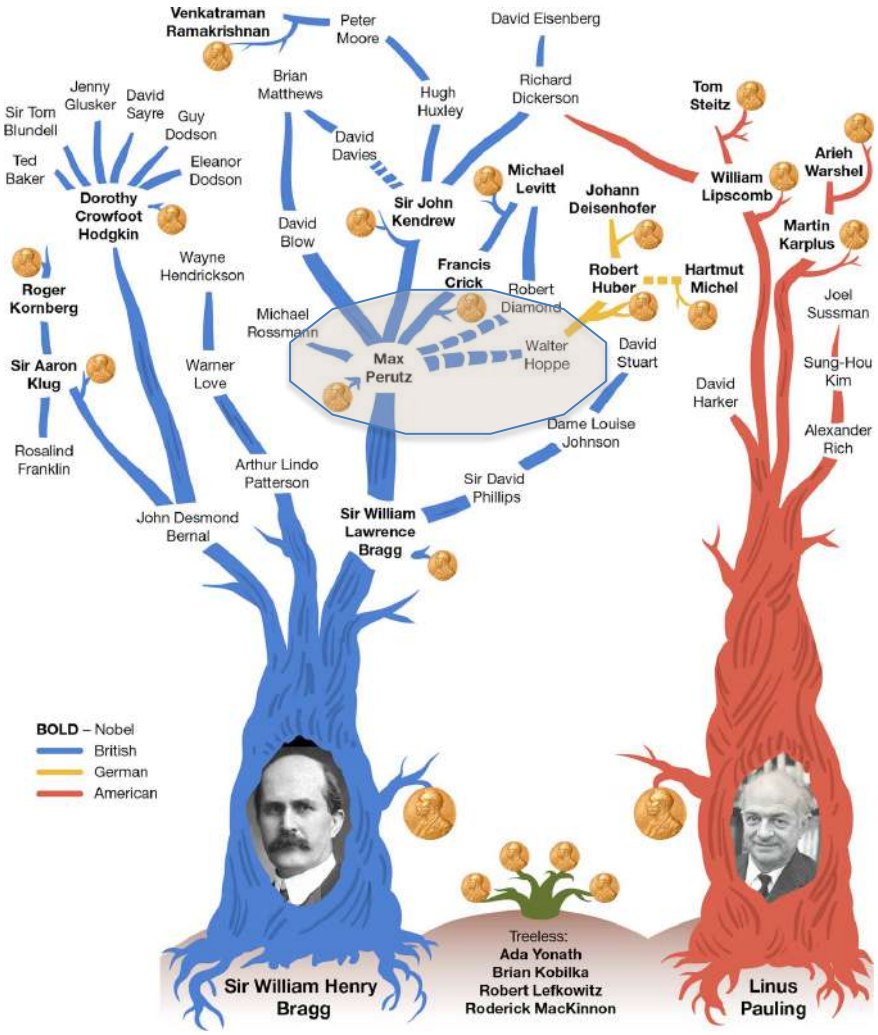

5% of all Nobel Prizes are related to X-ray crystallography. Half of these were for biomolecules

One of the first Hybrid Meetings!

Hirschegg, site of 1968 workshop on X-ray crystallography and EM of proteins organized by Walter Hoppe and Max Perutz.

Harold Erickson, Richard Henderson, Ken Holmes, Hugh Huxley, Nigel Unwin . . .

Conference site of the
Hirschegg Meetings

Walter Hoppe with Max Perutz
in Hirschegg

The First Electron Microscope (1931)

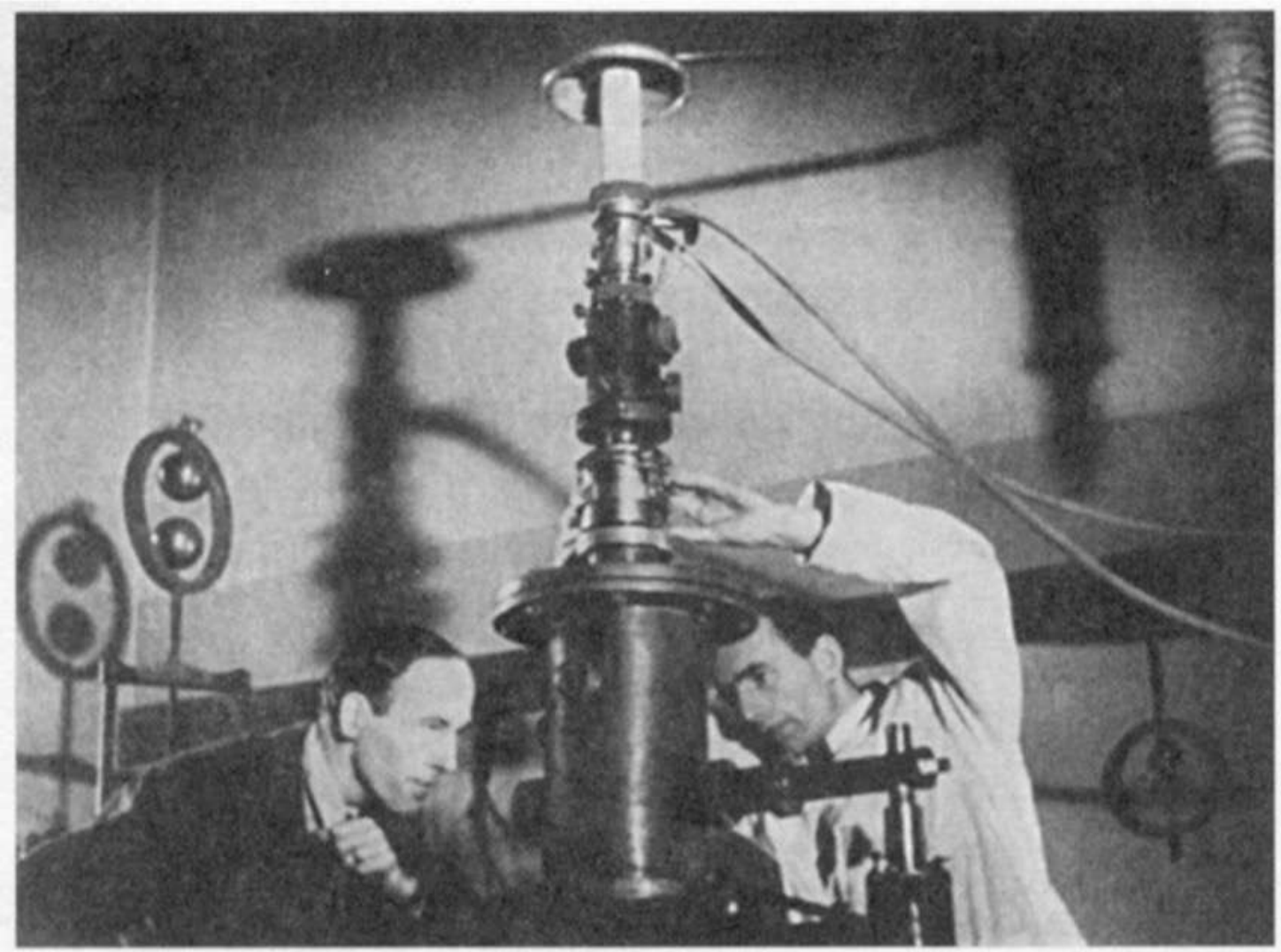

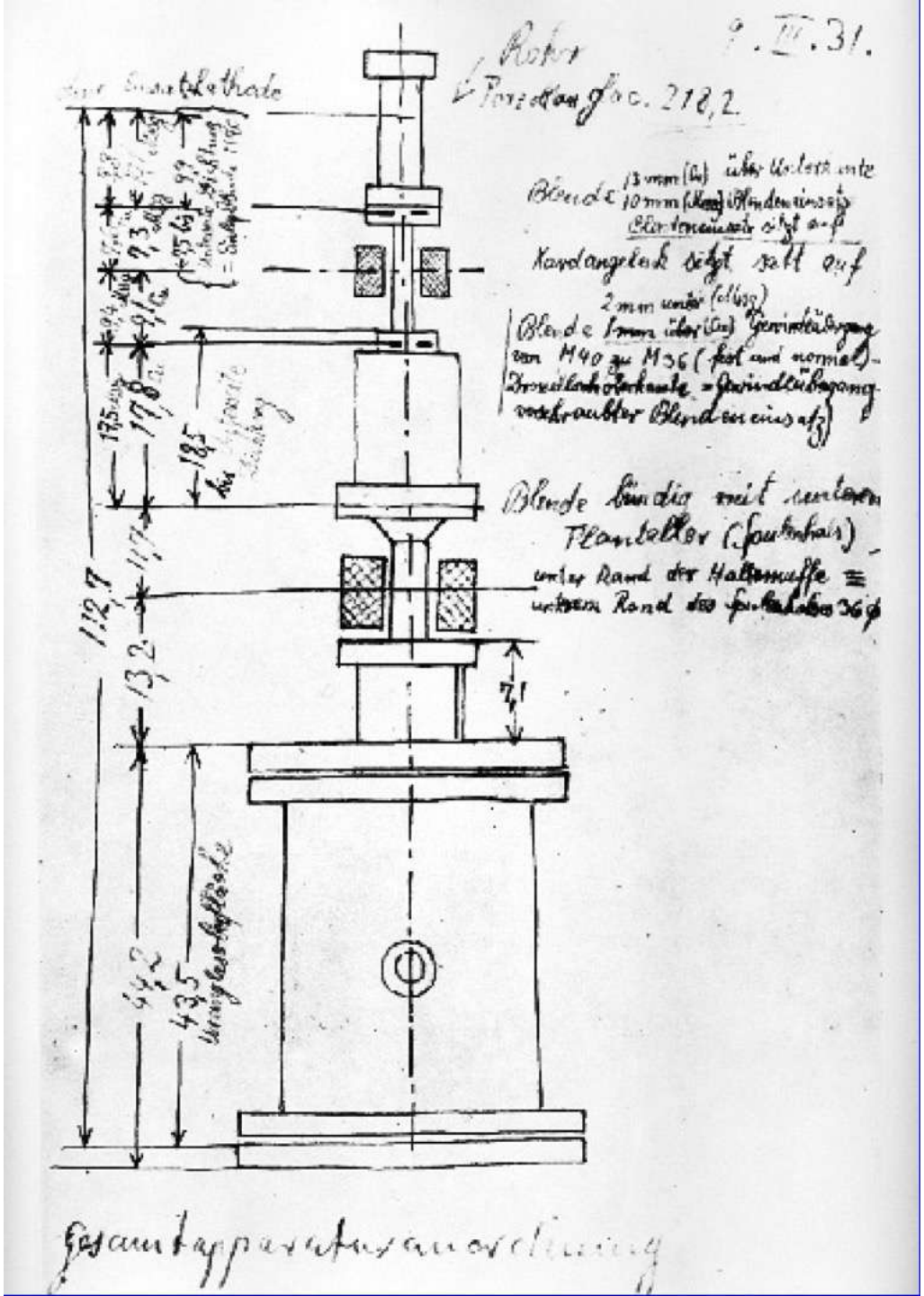

Ernst Ruska 1931 Nobel Prize in Physics in 1986

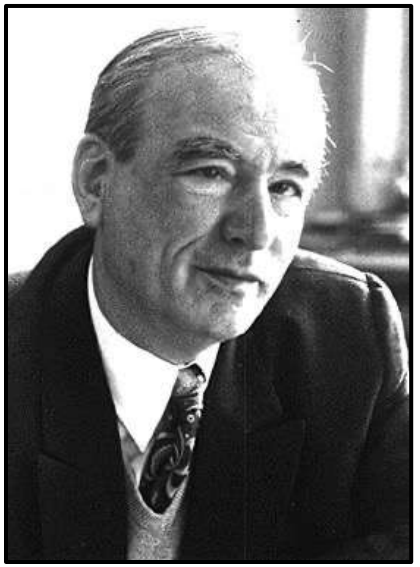

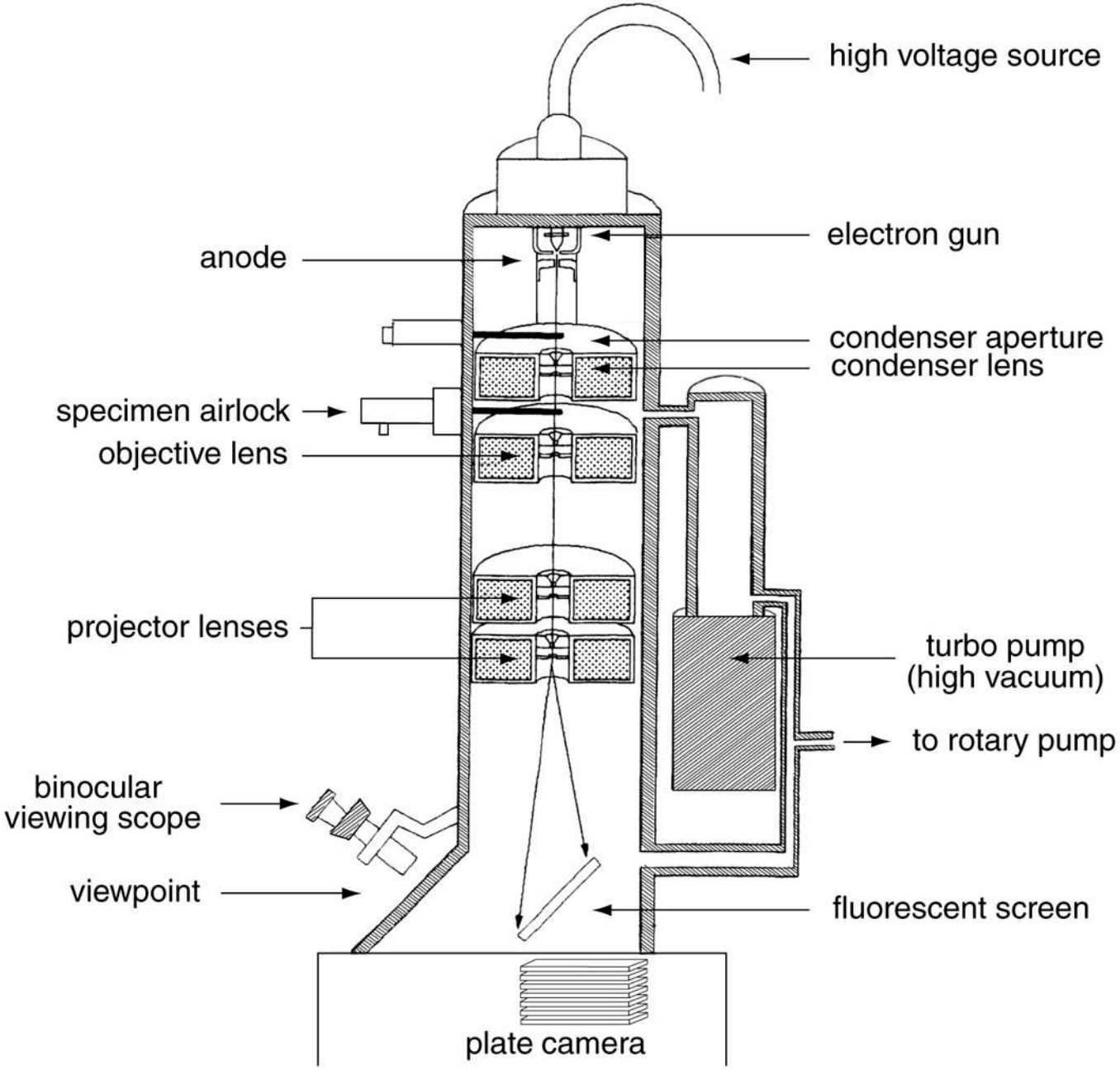
high voltage source
electron gun
anode
condenser aperture
condenser lens
specimen airlock
objective lens
projector lenses
turbo pump
(high vacuum)
to rotary pump
binocular
viewing scope
viewpoint
fluorescent screen
plate camera

USING ELECTRONS FOR IMAGING BIOLOGICAL MOLECULES

Basic incompatibility of biological imaging:

1) *Electrons destroy biological matter. "Shooting with cannons at sparrows"*

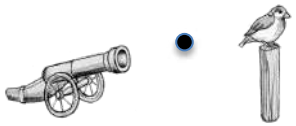

2) Electrons require vacuum to travel; biomolecules require an aqueous environment for their structure to be sustained

Solution:

low exposure

hydration chamber or *ice embedding*

→ Low exposure + averaging over many repeats of a molecule image

→ Hydration to keep molecule in native state: hydration chamber at room temperature
-- or -- embedding in vitreous ice, cryo-EM

Interactions of electrons with biological matter at 100 – 300 kV

- Elastic (high-res signal) vs. inelastic scattering (low-res, delocalized signal)
- Only the elastic component is useful for imaging
- Transmission electron microscopy: maximum thickness is ~0.25 μ = 2500 Å
- Larger thickness leads to multiple scattering and, eventually, total absorption

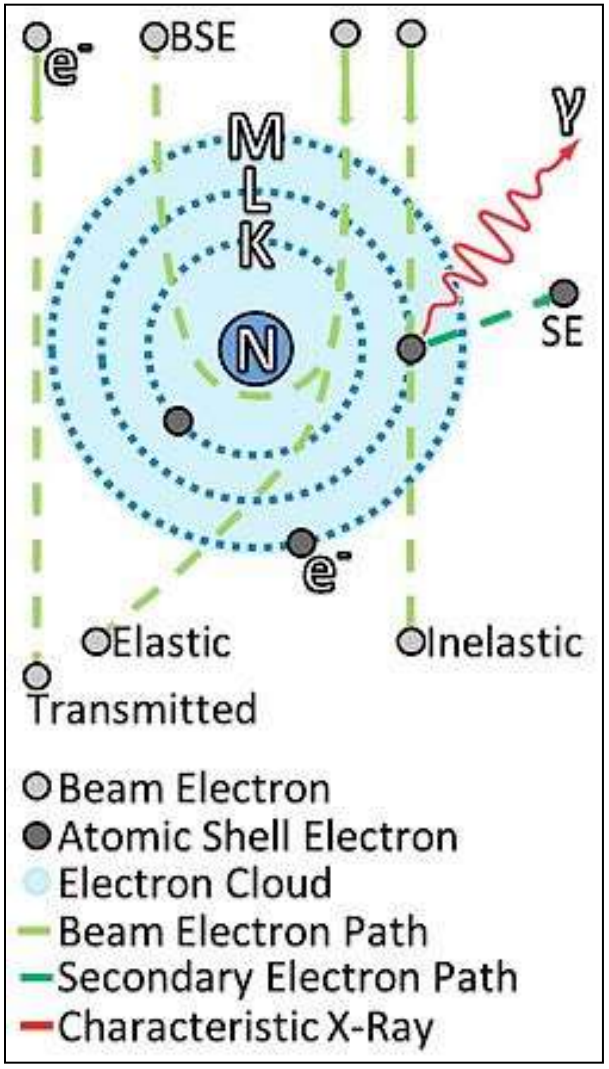

Visualization/Structure Determination by Transmission Electron Microscopy

- The transmission electron microscope can be used to solve molecular structures.
- *Projection images formed at very high magnification, e.g. 30,000 x.*
- To reconstruct an object, many different views must be collected.
- ☹ *Sample must be very thin, electrons are readily absorbed by matter.*
- ☹ Electrons strongly damage the molecules -- need for low dose! 10-20 electrons/square Angstrom.
- ☹ *Images are very noisy (shot noise)*
- ☹ Initially, negative staining needed to be used for sample preparation of molecules. Cryo-sample preparations were developed later.
-

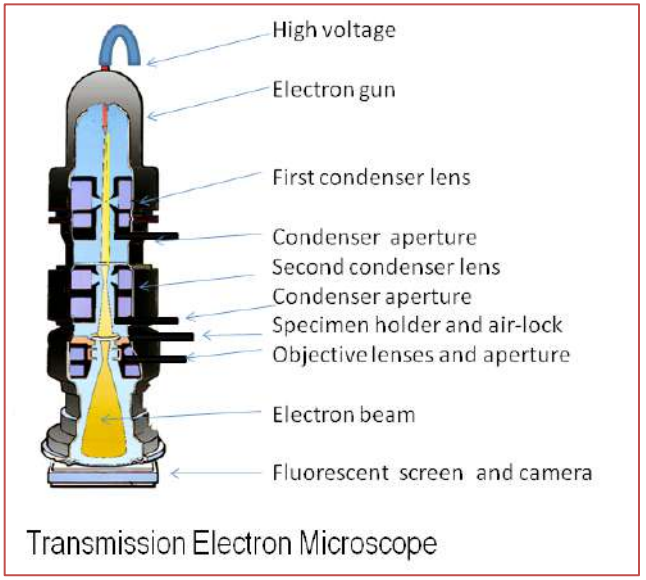

http://www.newworldencyclopedia.org/entry/File:Electron Microscope.png

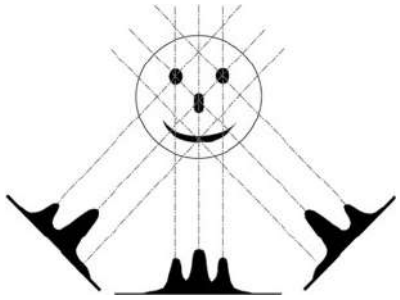

LOW EXPOSURE 1971

Journal of Ultrastructure Research
Volume 36, Issues 3–4, August 1971, Pages 466-482

Limitations to significant information biological electron microscopy as a result of radiation damage 1,

Robert M. Glaeser

Robert M. Glaeser

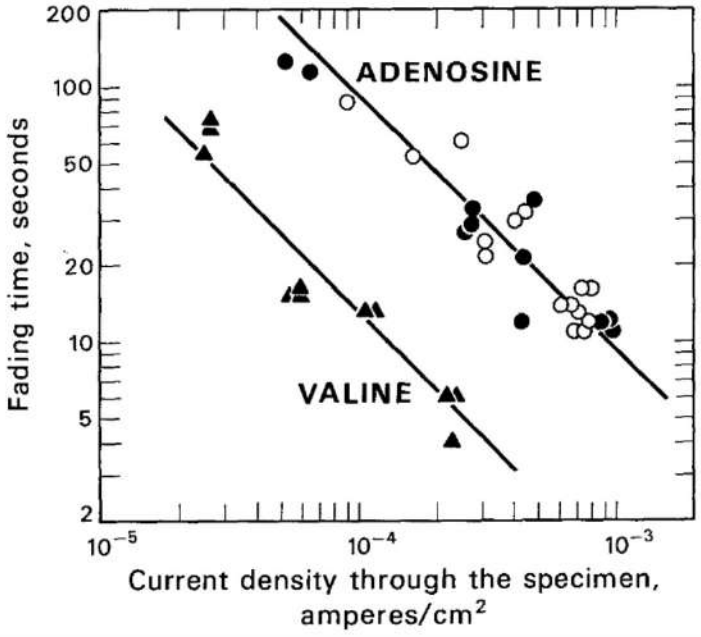

HYDRATION CHAMBER 1974

JOURNAL ARTICLE

Structure of Wet Specimens in Electron Microscopy

D. F. Parsons

Science
New Series, Vol. 186, No. 4162 (Nov. 1, 1974), pp. 407-414 (8 pages)
Published By: American Association for the Advancement of Science

https://www.jstor.org/stable/1739696

Donald F. Parsons

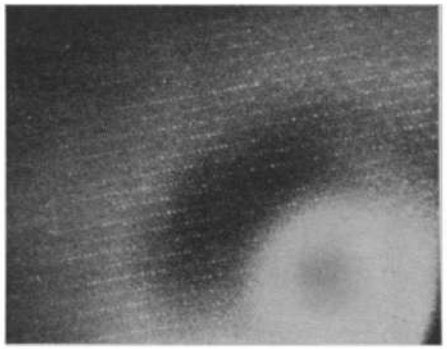

Fig. 3. Electron diffraction pattern of a wet microcrystal of ox liver catalase recorded on No-Screen medical x-ray film at 200 kv. The projection was $P2_1$-2_1 symmetry and corresponds to an orthorhombic habit of catalase.

PLUNGE FREEZING/EMBEDDING IN VITREOUS ICE 1981

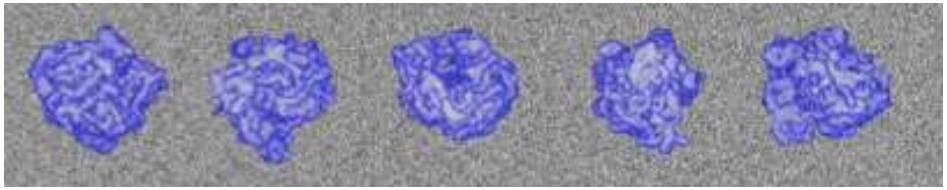

Molecules embedded in vitreous ice

Robert Glaeser
1976

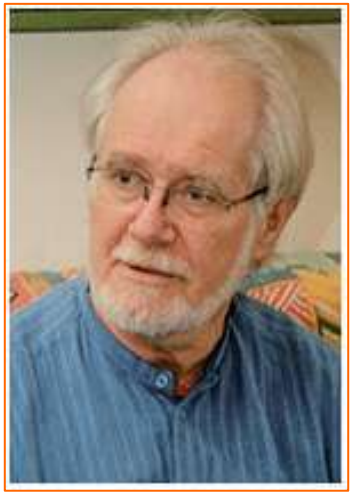

Jacques Dubochet
1981

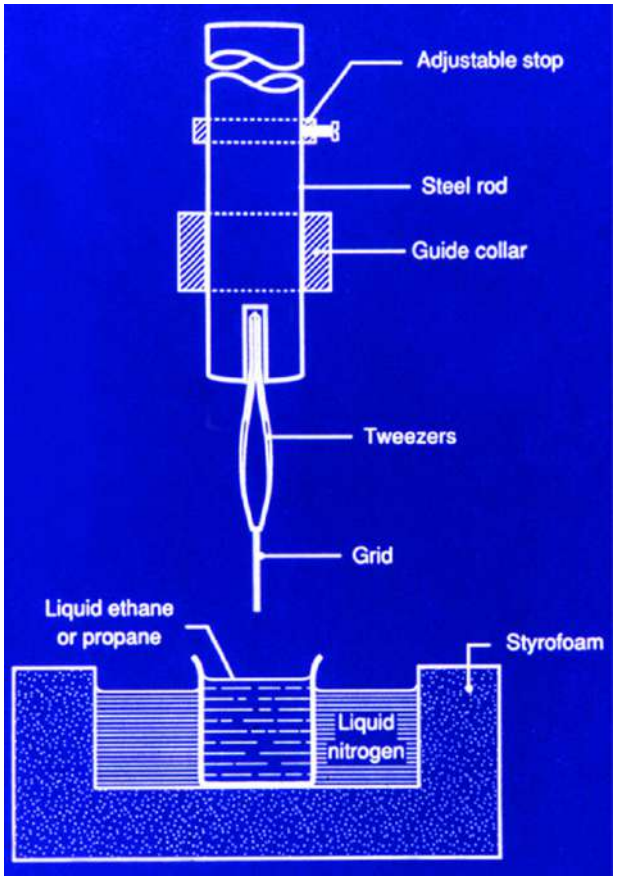

Plunge-freezer

3D RECONSTRUCTION

Among Radon's extensive work on calculus of variations, differential geometry and measure theory there is a paper appropriately titled

"Über die Bestimmung von Funktionen durch ihre Integralwerte längs gewisser Mannigfaltigkeiten." (1905)

It describes the way a multidimensional function is related to its projections, both in real and Fourier space.

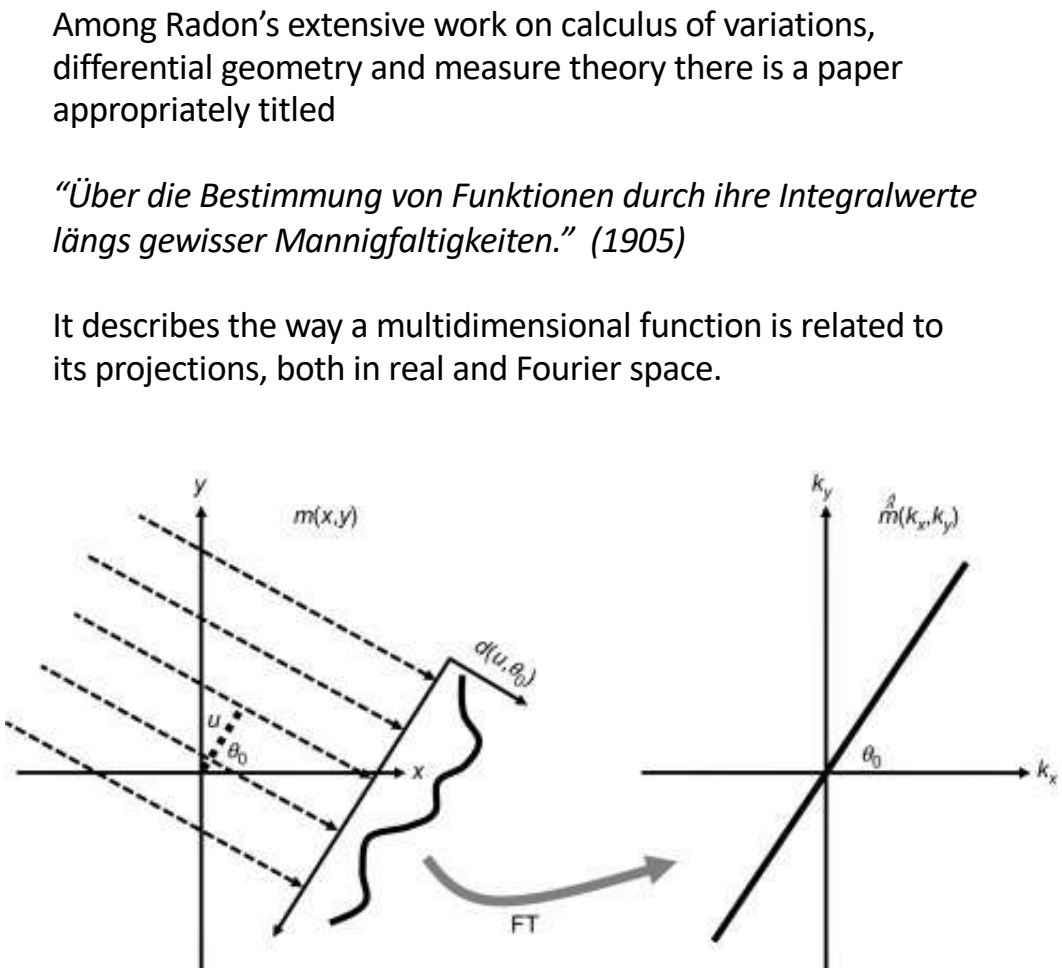

Johannes Radon
1887 - 1956

THREE-DIMENSIONAL RECONSTRUCTION:
STRUCTURES WITH HELICAL SYMMETRY. 1968
(sample prep: negative staining)

Pioneering work: 3D reconstruction of a bacteriophage tail using the Fourier-Bessel approach, 1968

Application of the Projection-Slice Theorem

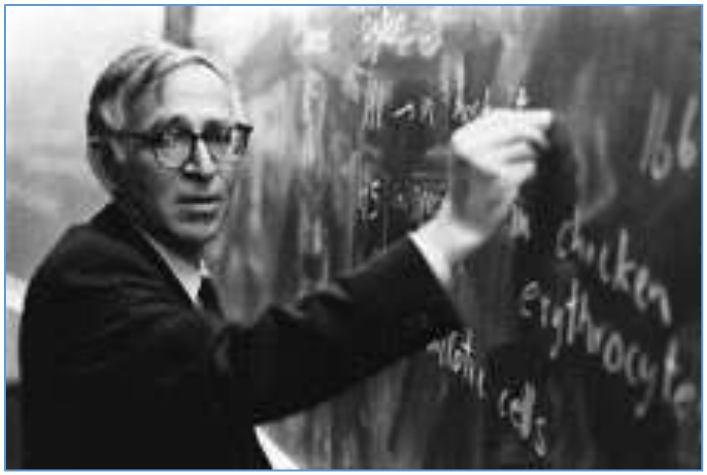

Aaron Klug and David DeRosier, LMB/MRC Cambridge

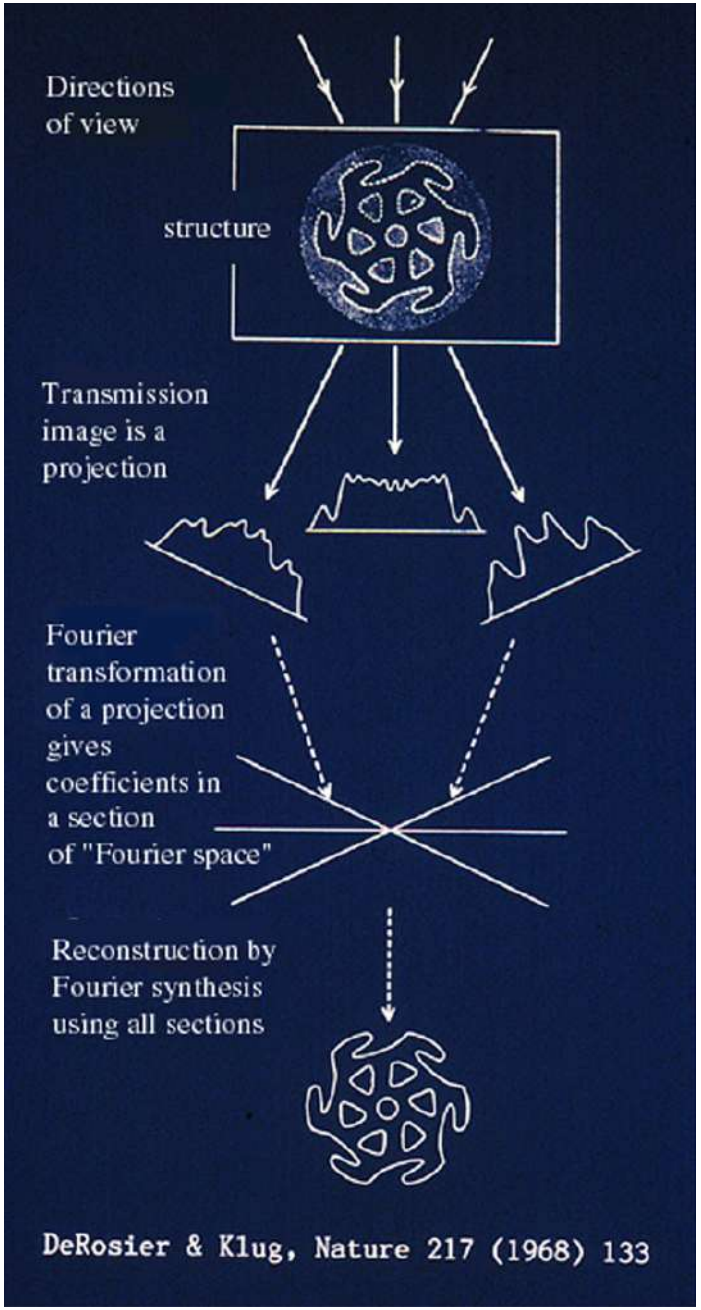

THREE-DIMENSIONAL RECONSTRUCTION: VIRUSES WITH ICOSAHEDRAL SYMMETRY (sample prep: negative staining) 1970

tomato bushy stunt virus

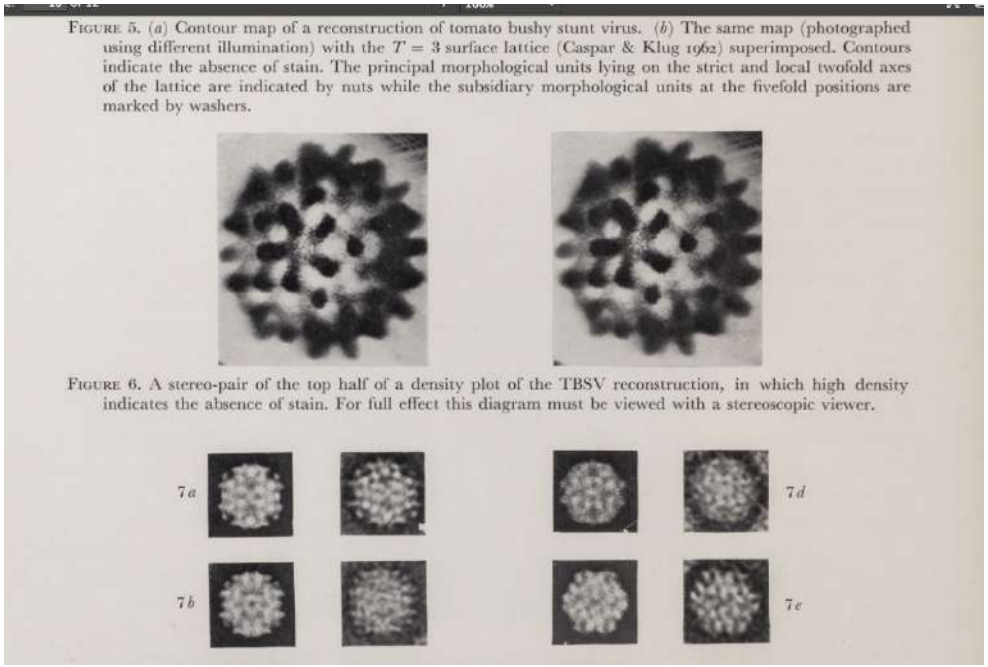

FIGURE 5. (*a*) Contour map of a reconstruction of tomato bushy stunt virus. (*b*) The same map (photographed using different illumination) with the $T = 3$ surface lattice (Caspar & Klug 1962) superimposed. Contours indicate the absence of stain. The principal morphological units lying on the strict and local twofold axes of the lattice are indicated by nuts while the subsidiary morphological units at the fivefold positions are marked by washers.

FIGURE 6. A stereo-pair of the top half of a density plot of the TBSV reconstruction, in which high density indicates the absence of stain. For full effect this diagram must be viewed with a stereoscopic viewer.

7*a* 7*d* 7*b* 7*e*

R. A. Crowther, Phil. Trans. Roy. Soc. 1971

Tony Crowther

THREE-DIMENSIONAL RECONSTRUCTION: STRUCTURES THAT FORM 2D CRYSTALS (glucose embedding). 1975

(Reprinted from Nature, Vol. 257, No. 5521, pp. 28–32, September 4, 1975)

Plants don't [illegible]

Three-dimensional model of purple membrane obtained by electron microscopy

R. Henderson & P. N. T. Unwin

MRC Laboratory of Molecular Biology, Hills Road, Cambridge CB2 2QH, UK

A 7-Å resolution map of the purple membrane has been obtained by electron microscopy of tilted, unstained specimens. The protein in the membrane contains seven, closely packed, α-helical segments which extend roughly perpendicular to the plane of the membrane for most of its width. Lipid bilayer regions fill the spaces between the protein molecules.

The purple membrane is a specialised part of the cell membrane of *Halobacterium halobium*[1]. Oesterhelt and Stoeckenius[2] have shown that it functions *in vivo* as a light-driven hydrogen ion pump involved in photosynthesis. It contains identical protein molecules of molecular weight 26,000, which make up 75% of the total mass, and lipid which makes up the remaining 25% (ref. 3). Retinal, covalently linked to each protein molecule in a 1:1 ratio is responsible for the characteristic purple colour[2]. These components together form an extremely regular two-dimensional array[4].

We have studied the purple membrane by electron microscopy using a method for determining the projected structures of unstained crystalline specimens[5]. By applying the method to tilted specimens, and using the principles put forward by De Rosier and Klug[6] for the combination of such two-dimensional views, we have obtained a three-dimensional map of the membrane at 7 Å resolution. The map reveals the location of the protein and lipid components, the arrangement of the polypeptide chains within each protein molecule, and the relationship of the protein molecules in the lattice.

Electron microscopy and diffraction

The purple membrane was prepared under normal conditions from cultures of *H. halobium*[3] and applied to the microscope grid in the presence of 0.5% glucose. The purified membranes are mostly oval sheets up to 1.0 μm in diameter and about 45 Å thick[4,7]. The array of molecules making up these sheets is accurately described[7] as an almost perfect crystal of space group P3 ($a = 62$ Å) with a thickness of one unit cell only in the direction of the c axis. A single membrane thus contains up to 40,000 unit cells; that is 120,000 protein molecules (three per unit cell).

These large periodic arrays from which electron diffraction patterns and defocused bright field micrographs are recorded[5] enable us to overcome the principal problem normally associated with high resolution electron microscopy of unstained biological materials; that is, sensitivity to electron damage[8]. Only a small number of electrons can pass through each unit cell before it is destroyed, but because of the large number of unit cells, the information in the diffraction patterns and micrographs is sufficient to provide a picture of the average unit cell. The micrographs recorded with such low doses of electrons appear featureless, since the statistical fluctuation in the number of electrons striking the plate is large compared with the weak phase contrast (< 1%) produced by defocusing.

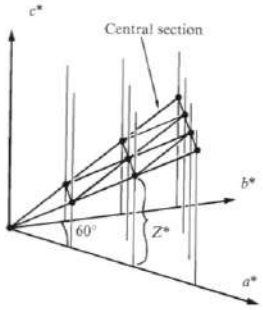

Fig. 1 Part of the three-dimensional reciprocal lattice showing the geometry of the lattice lines in the hexagonal space group P3. a^*, b^* and c^* are the reciprocal lattice vectors. a^* and b^* lie in, and c^* is perpendicular to the plane of the membrane. A central section which is perpendicular to the incident electron beam has been drawn through the lattice. The intersection of this central section with the reciprocal lattice is determined by the angle of tilt and the axis about which the membrane is tilted. Individual diffraction patterns and micrographs provide the amplitudes and phases in this section at the points shown. z^* represents the coordinate along the c^* direction of one of the points. The angle of tilt was measured to within 2° for each of the specially modified, tilted specimen holders, and the direction of the tilt axis on the photographic plate was established during operation of the microscope. However, estimates based on the geometry of the spacings of the lattice points (for high tilt angles), the variation of the degree of underfocus across the plate (for low tilt angles), and least squares refinement against data obtained at high tilt angles (for diffraction patterns) provided more accurate figures which were used in the calculation. The accuracy of measurement of both the amplitudes and phases depended on having sharp lattice lines. We therefore took care to ensure that, on the microscope grid, the membranes remained coherently ordered and flat to within 1/5°.

As a result, analysis of each micrograph by densitometry and computer processing[8] is required to combine the information from individual unit cells.

Solution of the three-dimensional structure of the purple membrane requires the determination of the amplitudes and phases in three dimensions of the Fourier terms into which it can be analysed. The diffraction pattern or Fourier transform of the membrane is not a three-dimensional lattice of points as is the case with a normal crystal, but since it is only one unit cell thick, a two-dimensional lattice of lines which are continuous in the direction of c^* (that is perpendicular to the membrane). A single electron diffraction experiment therefore

Richard Henderson and Nigel Unwin

Purple membrane
Protein

Bacteriorhodopsin

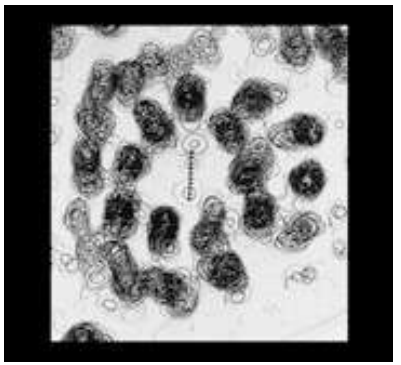

<u>Electron dose is spread over many repeats of the molecule in the crystal</u>

Why Crystals?
3D Reconstruction of Asymmetrical Molecules by Electron Tomography ~1968

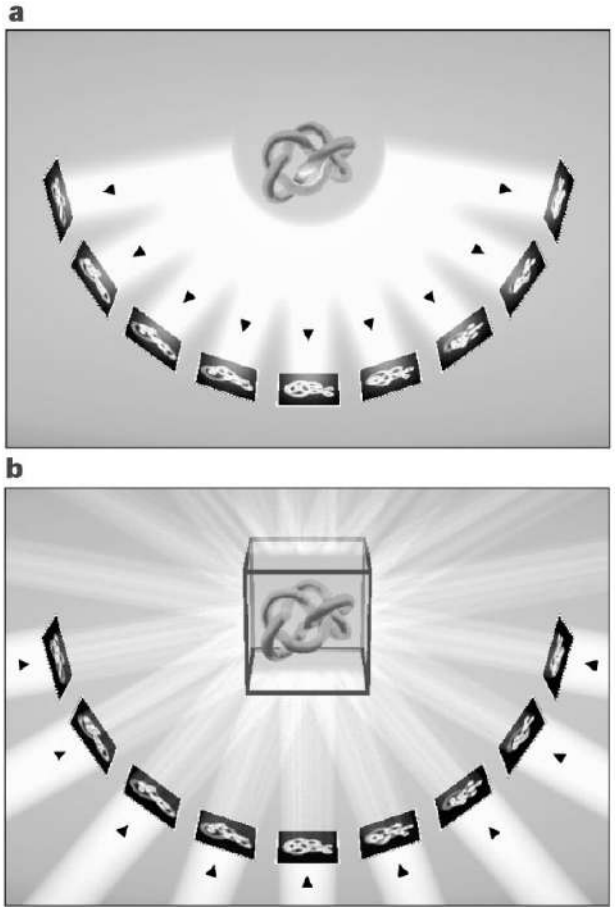

- Electron Tomography of single molecules
- Examples: fatty acid synthetase and ribosome
- BUT: Accumulated electron exposure exceeded 1000 e^-/A^2

Walter Hoppe (MPG Archive)

Why Crystals?
3D Reconstruction of Asymmetrical Molecules by Single-Particle Techniques – the Concept 1975

- Single-particle techniques: structural information from images of single (i.e., unattached) molecules in many copies.
- *Molecules are free to assume all naturally occurring conformations.*
- Molecules are randomly oriented.
- *A single snapshot may already give us hundreds of particle views.*
- As we collect more snapshots, more orientations will be covered, until we have enough for reconstructing the molecule in three dimensions.
-

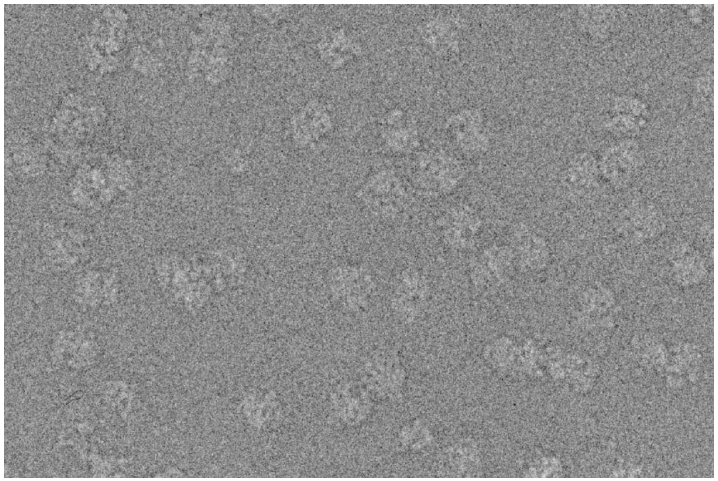

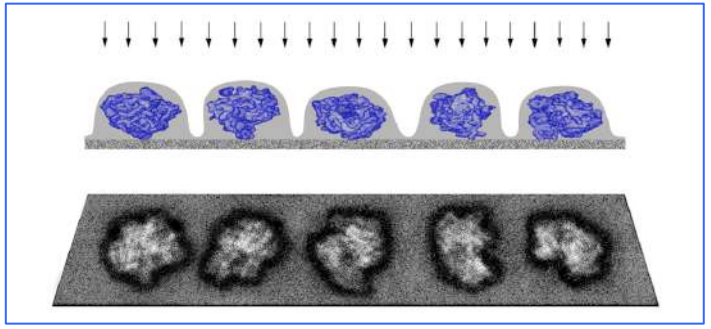

EM images can be aligned to within better than 3 Angstrom!

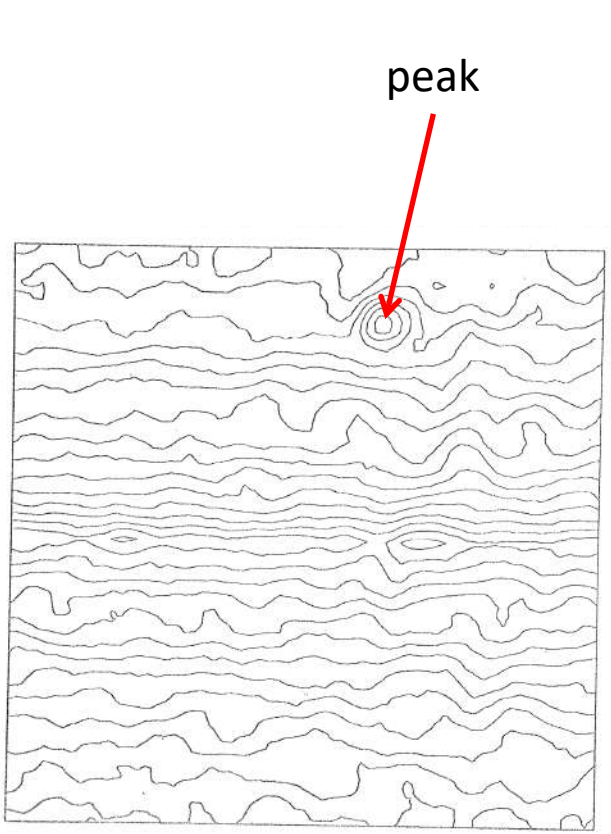

. 11a,b Graphitfolie; Korrelationsfunktionen
ßer Teilbereich). Höhenschichtlinien:
Abstand 0.006, von 0.0 bis 0.03
Abstand 0.001, von 0.147 bis 0.166

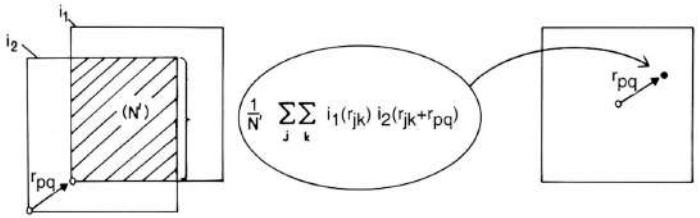

Fig. 3.8. Definition of the cross-correlation function. Image 1 is shifted with respect to image 2 by vector $\mathbf{r}_{pq}$. In this shifted position, the scalar product of the two images arrays is formed and put into the CCF matrix at position (p, q). The vector $\mathbf{r}_{pq}$ is now allowed to assume all positions on the sampling grid. In the end, the CCF matrix has an entry in each position. From Frank (1980). Reproduced with permission of Springer-Verlag, New York.

Cross-correlation function of
2 successive micrographs
of the same carbon film

J. Frank, Ph.D. thesis 1970

Dissertation at
Technical University Munich,
published in 2019,
49 years after completion

J. Frank (1970) “Analysis of high-resolution electron micrographs using image difference and reconstruction methods”

Ultramicroscopy 1 (1975) 159–162

SHORT NOTE

AVERAGING OF LOW EXPOSURE ELECTRON MICROGRAPHS OF NON-PERIODIC OBJECTS

Joachim FRANK *
The Cavendish Laboratory, Free School Lane, Cambridge CB2 3RQ, UK

Received 20 October 1975

The investigation concerns the possibility of extending to non-periodic objects the low exposure averaging techniques recently proposed for non-destructive electron microscopy of periodic biological objects. Two methods are discussed which are based on cross-correlation and are in principle suited for solving this problem.

1. Introduction

Recent work on low exposure techniques combined with averaging [1–3] (called 'SNAP shot techniques' in [3]) shows that information can be retrieved from periodic biological objects at higher than conventionally available resolutions [4]. Unwin and Henderson [2] were able to achieve 7 Å image resolution, by re-6]. In these applications, the contrast of the individual marker atom image to be superposed is sufficient for straightforward alignment. However, the requirement of subminimum exposure poses a new problem: the alignment of features that are only faintly visible on a noisy background.

Conditions for alignment of two images of a molecule of size *D*

$$D \geq \frac{3}{c^2 dp_{crit}}$$

PARTICLE SIZE > 3 / [CONTRAST^2 x RESOLUTION (in Å) x CRITICAL ELECTRON DOSE]

Saxton & Frank, Ultramicroscopy 1977

Devil in the detail – *Problems to be solved:*

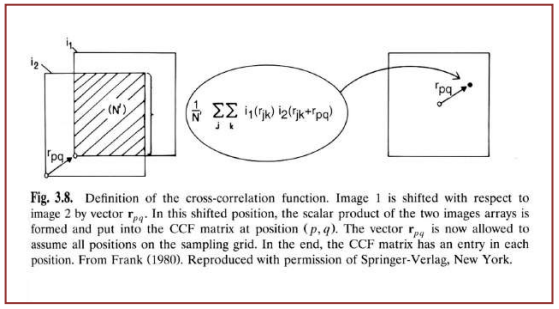

Fig. 3.8. Definition of the cross-correlation function. Image 1 is shifted with respect to image 2 by vector $\mathbf{r}_{pq}$. In this shifted position, the scalar product of the two images arrays is formed and put into the CCF matrix at position (p, q). The vector $\mathbf{r}_{pq}$ is now allowed to assume all positions on the sampling grid. In the end, the CCF matrix has an entry in each position. From Frank (1980). Reproduced with permission of Springer-Verlag, New York.

- ALIGN IMAGES
- CTF CORRECTION
- SORT/CLASSIFY IMAGES
- FIND PROJECTION ANGLES
- RECONSTRUCT IN 3D

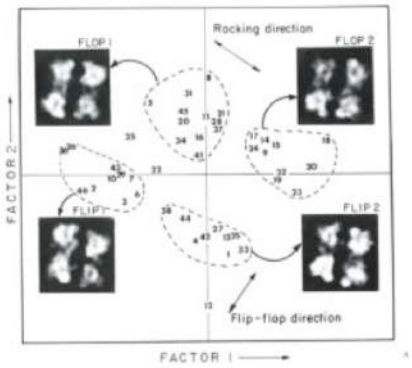

SPIDER -- Modular image processing program

Toronto EM conference abstract 1978
Ultramicroscopy 1981

Some of the operations
(out of hundreds):

AC -- autocorrelation
CC – cross-correlate 2 images
FT -- Fourier transform
RT -- rotate
SH -- shift
WI -- window

“WORKBENCH” FOR PROCESSING IMAGES

The Ribosome – its role in the development of Single-Particle Techniques

1927 - 1994

Miloslav Boublik
Roche Institute, Nutley, NJ

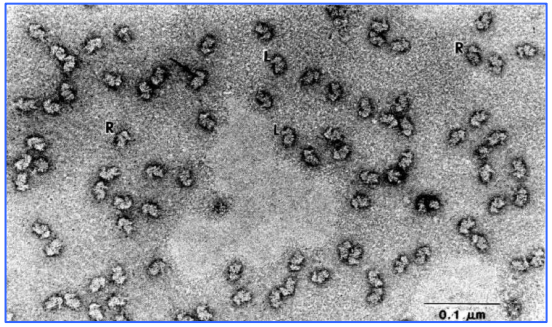

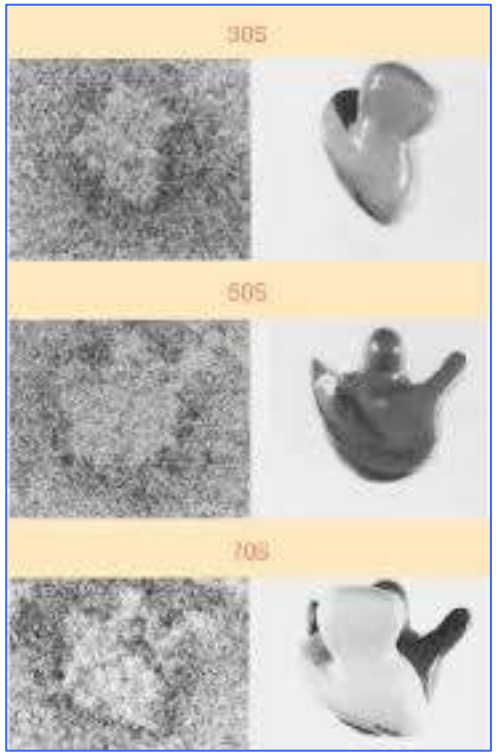

Jim Lake

In the beginning, there was the Lake model:
3D reconstruction by eye,
inferred from EM images

1970s

Alignment and averaging of single-particle images

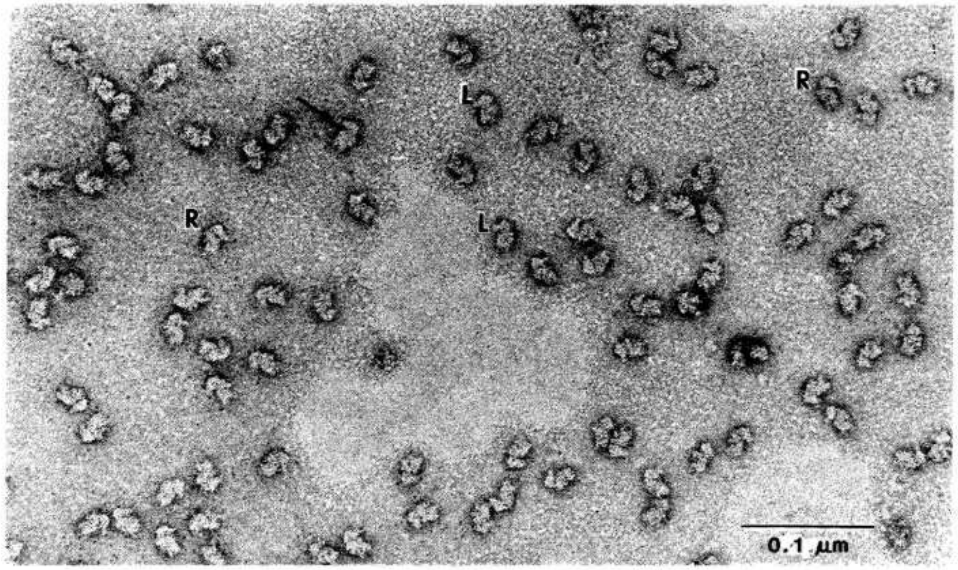

Proof of concept

40S subunits of HeLa (human) Ribosomes

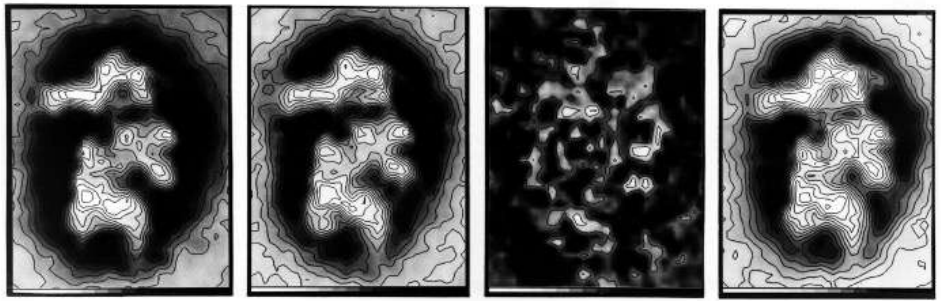

HALF-AVERAGES S.D. MAP AVERAGE

Frank et al., Science 1981

Problem of heterogeneity: molecules are in different orientations and conformations

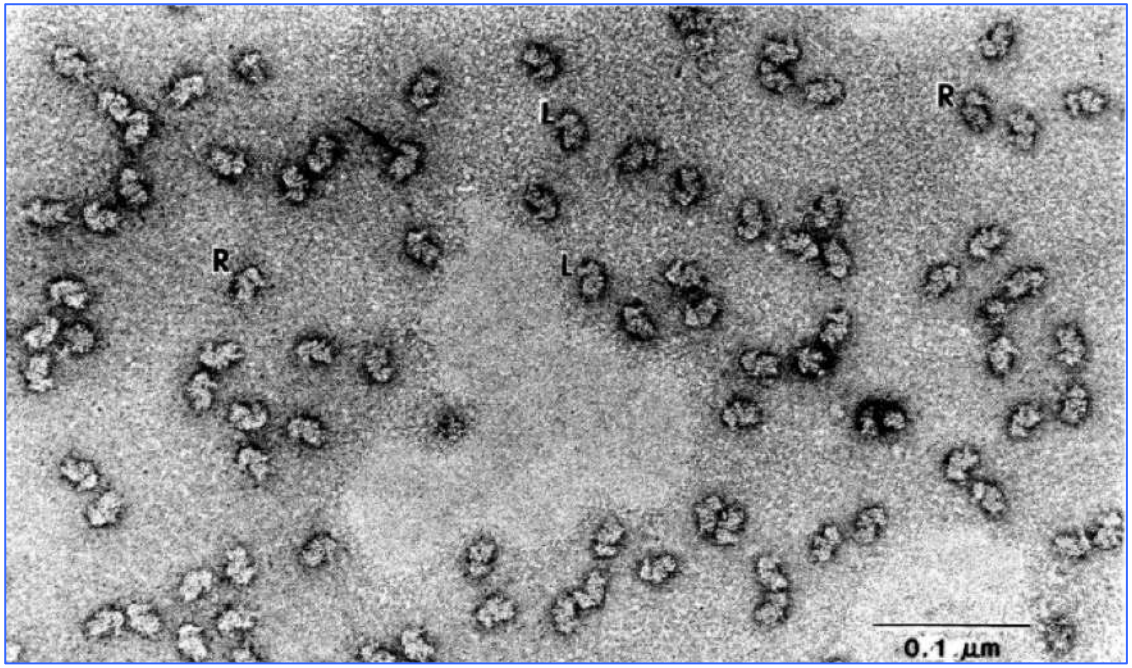

Frank et al., Science 1981

L and R views (flip and flop) of HeLa ribosomes

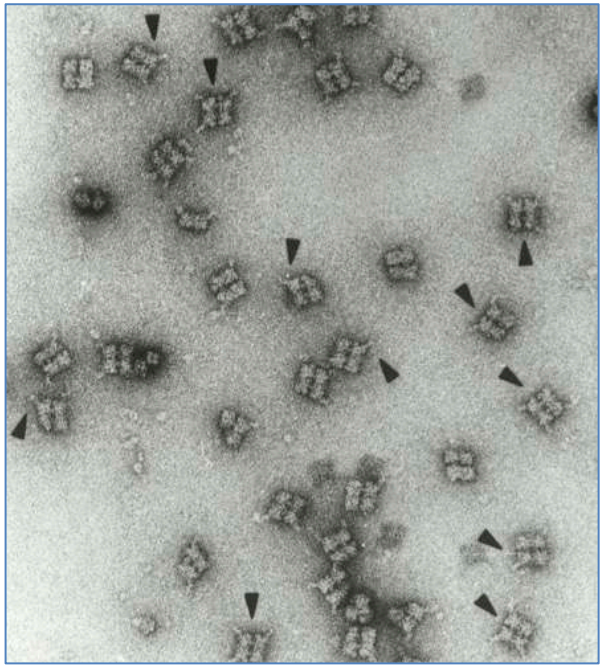

N. Boisset, thesis 1987

flip and flop views of hemocyanin

Multivariate analysis of aligned molecule images

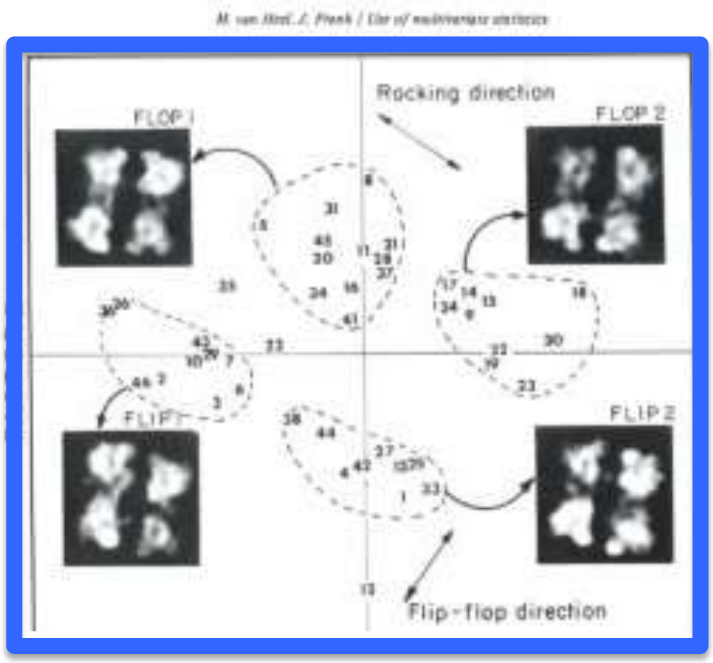

Van Heel and Frank, Ultramicroscopy 1981

FLIP/FLOP and Rocking positions

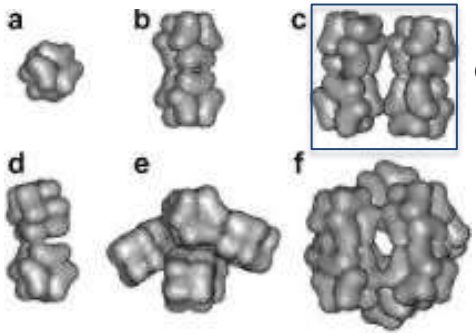

dodecamer

Hemocyanins of Arthropods are oligomers of a basic unit

How to Find the Angles of Projection

Via bootstrap:

Random-conical tilt reconstruction

1979 

1986/87 

Random-Conical Tilt Reconstruction (Principle)

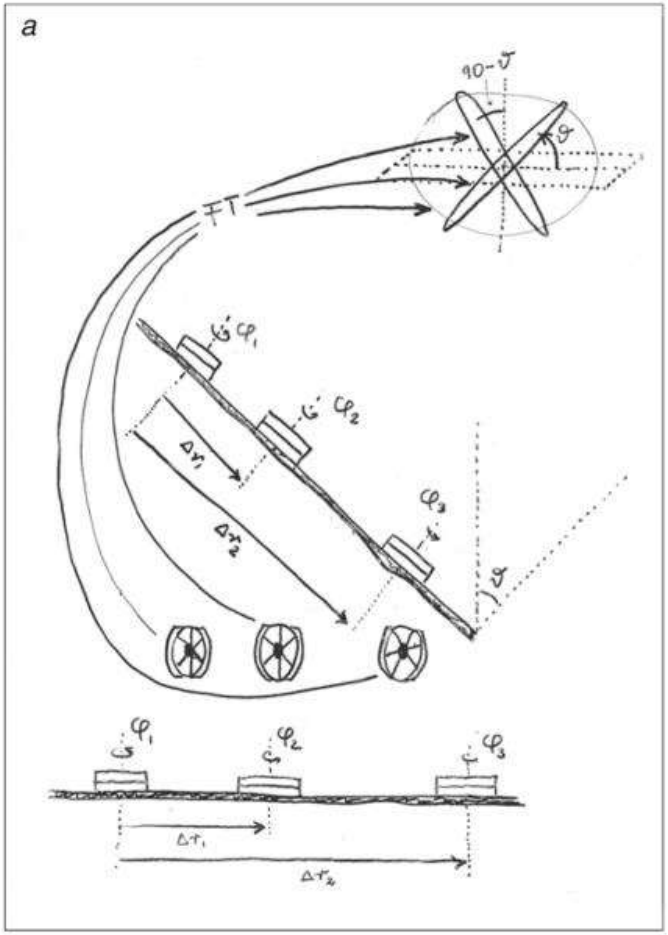

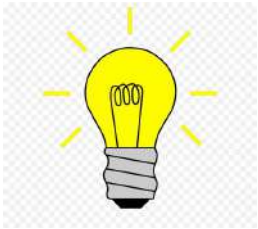

J. Frank, overhead 1979

Random-Conical Tilt Reconstruction (Principle – Fancy Version)

J. Frank, American Scientist 1998

First single-particle 3D reconstruction 1987

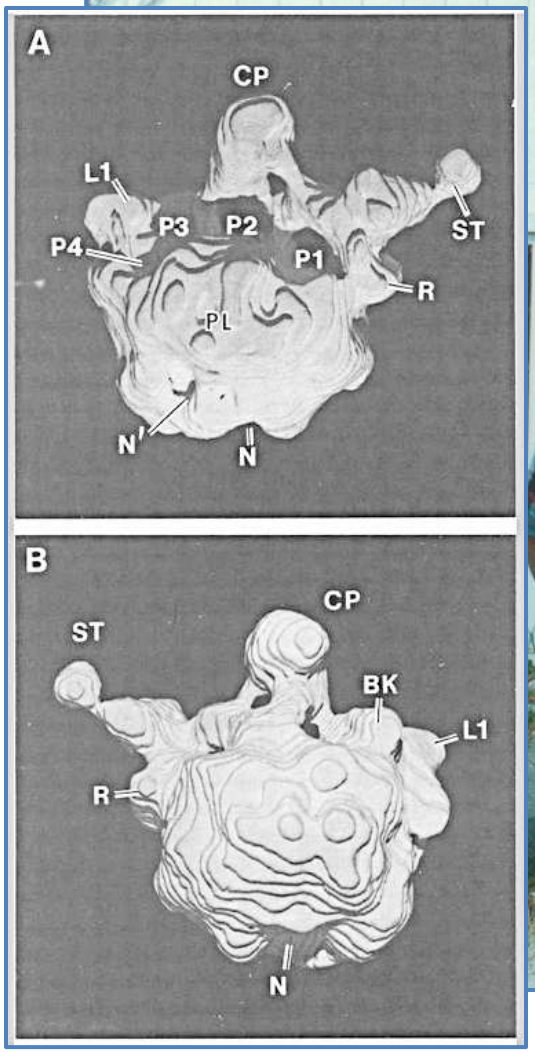

Michael Radermacher

Radermacher et al., EMBO J. 1987

The 50S ribosomal subunit
as a contour stack in 3D

First 3D Reconstruction using Single Particle Reconstruction
Nobel Museum, Stockholm

Frozen-hydrated specimens / Plunge-freezing / Vitreous ice / Cryo-EM

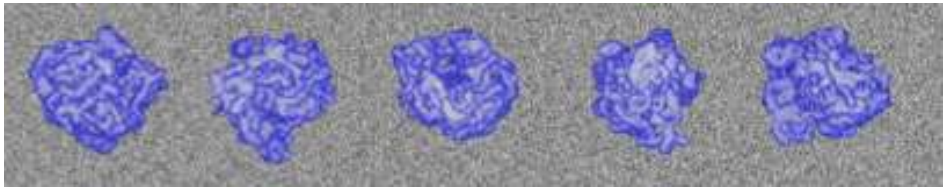

Molecules embedded in vitreous ice

Robert Glaeser
1976

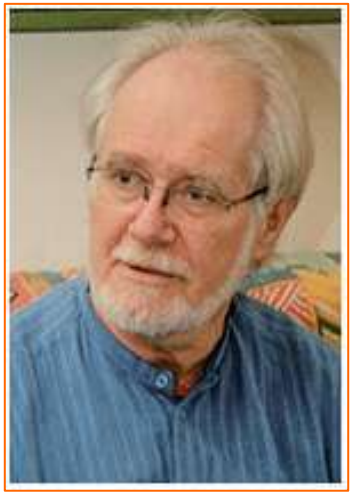

Jacques Dubochet
1981

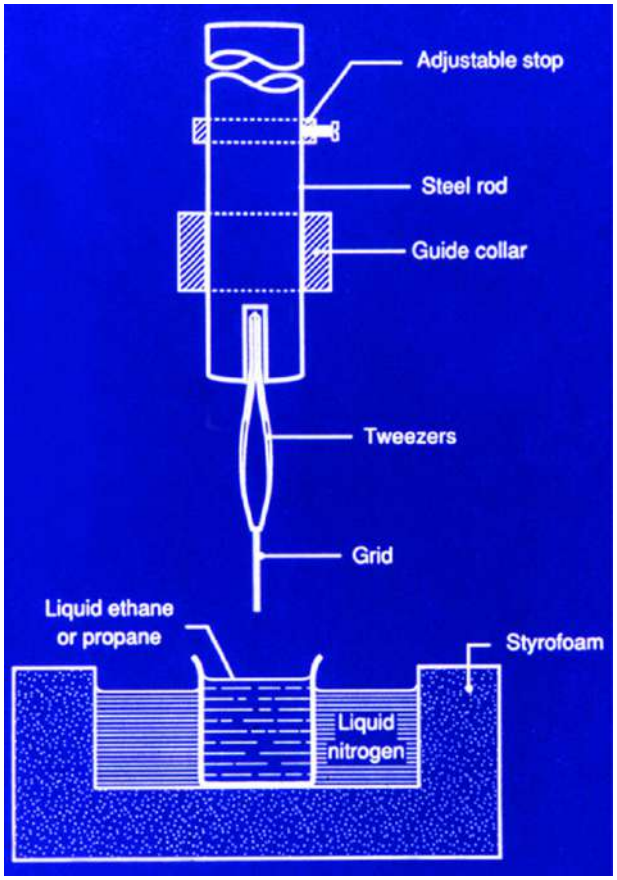

Plunge-freezer

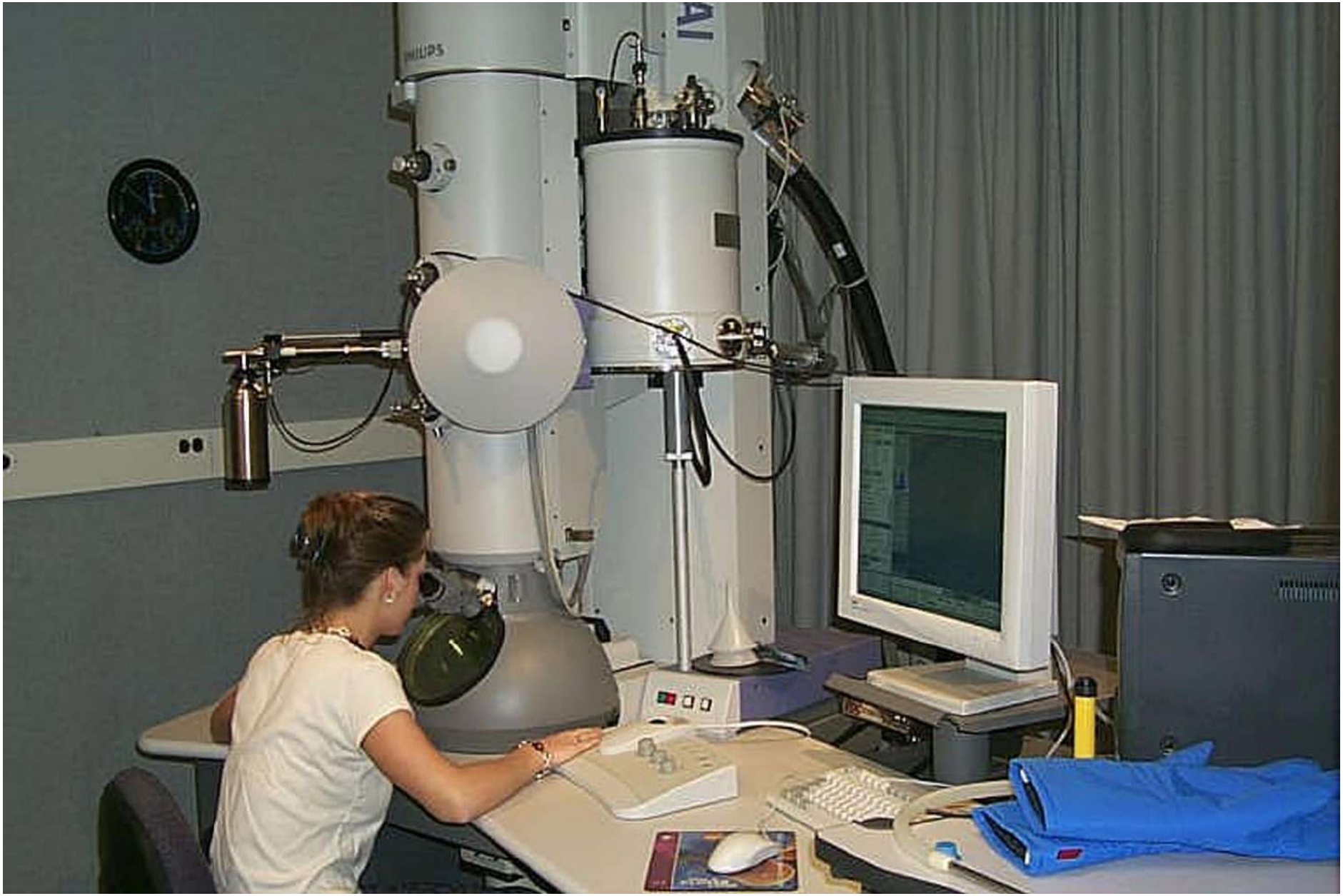

F30 Polara (FEI)

Plunge-freezers

---------- manual --------- ---------- automated, climatized ----------

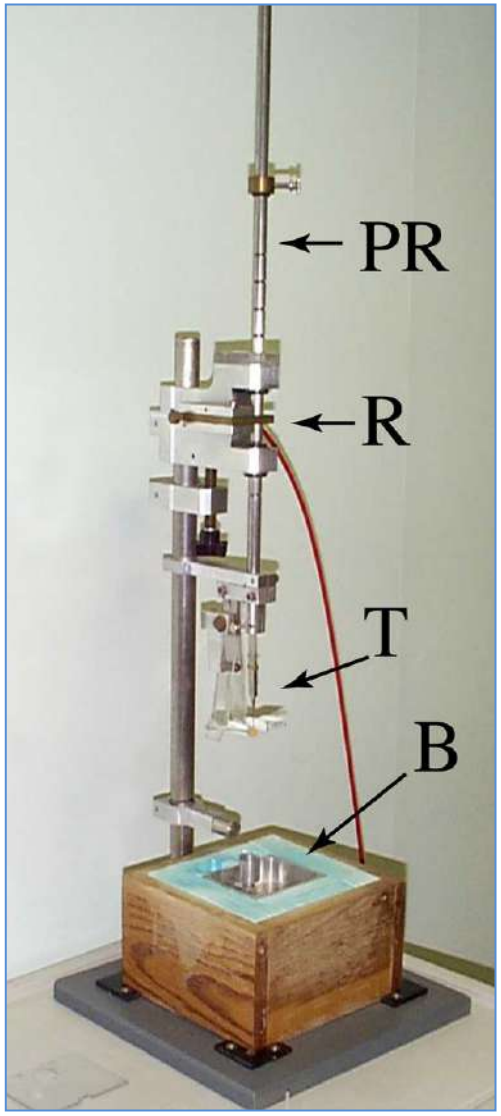

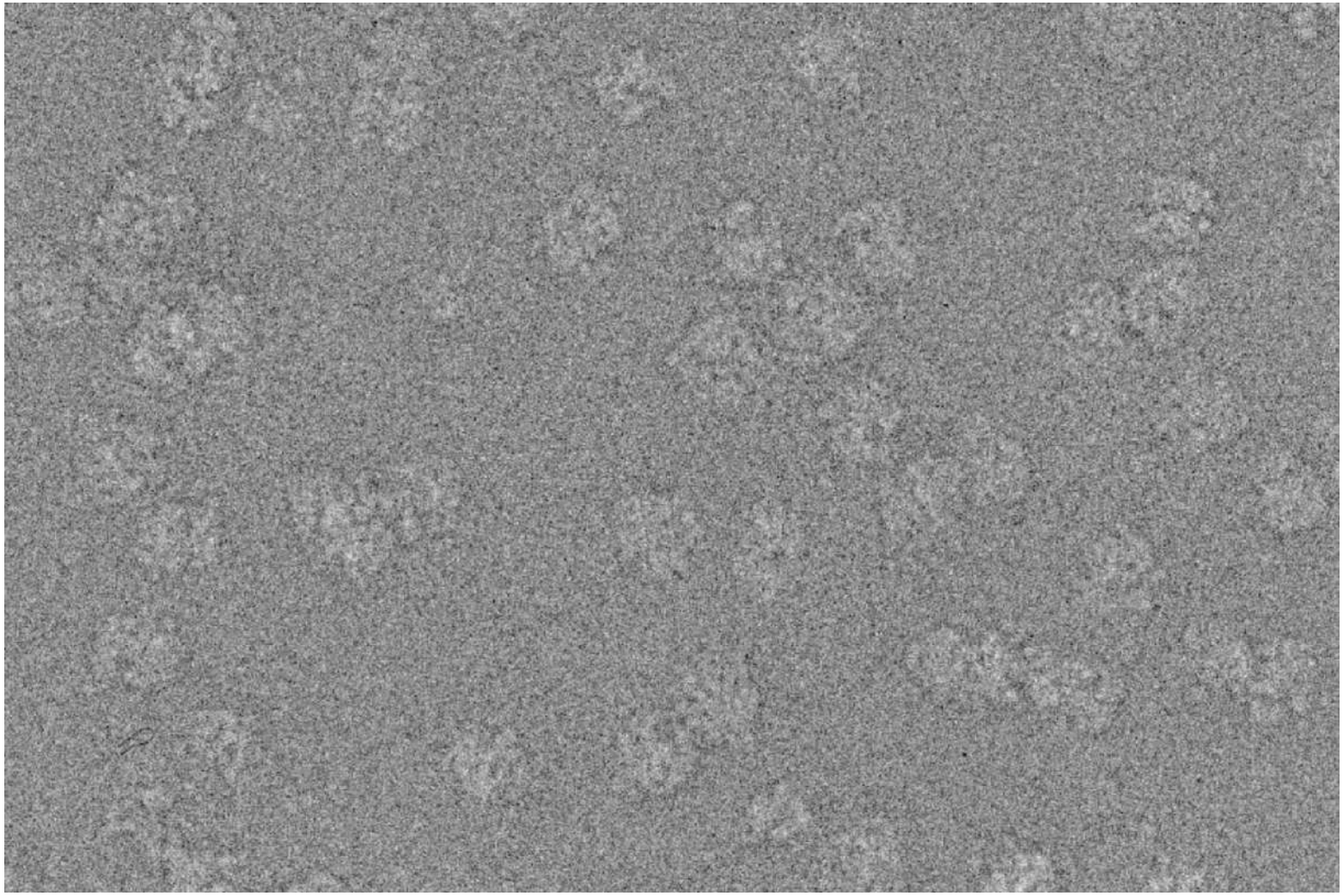

ribosomes, recorded on film

Iterative angular refinement

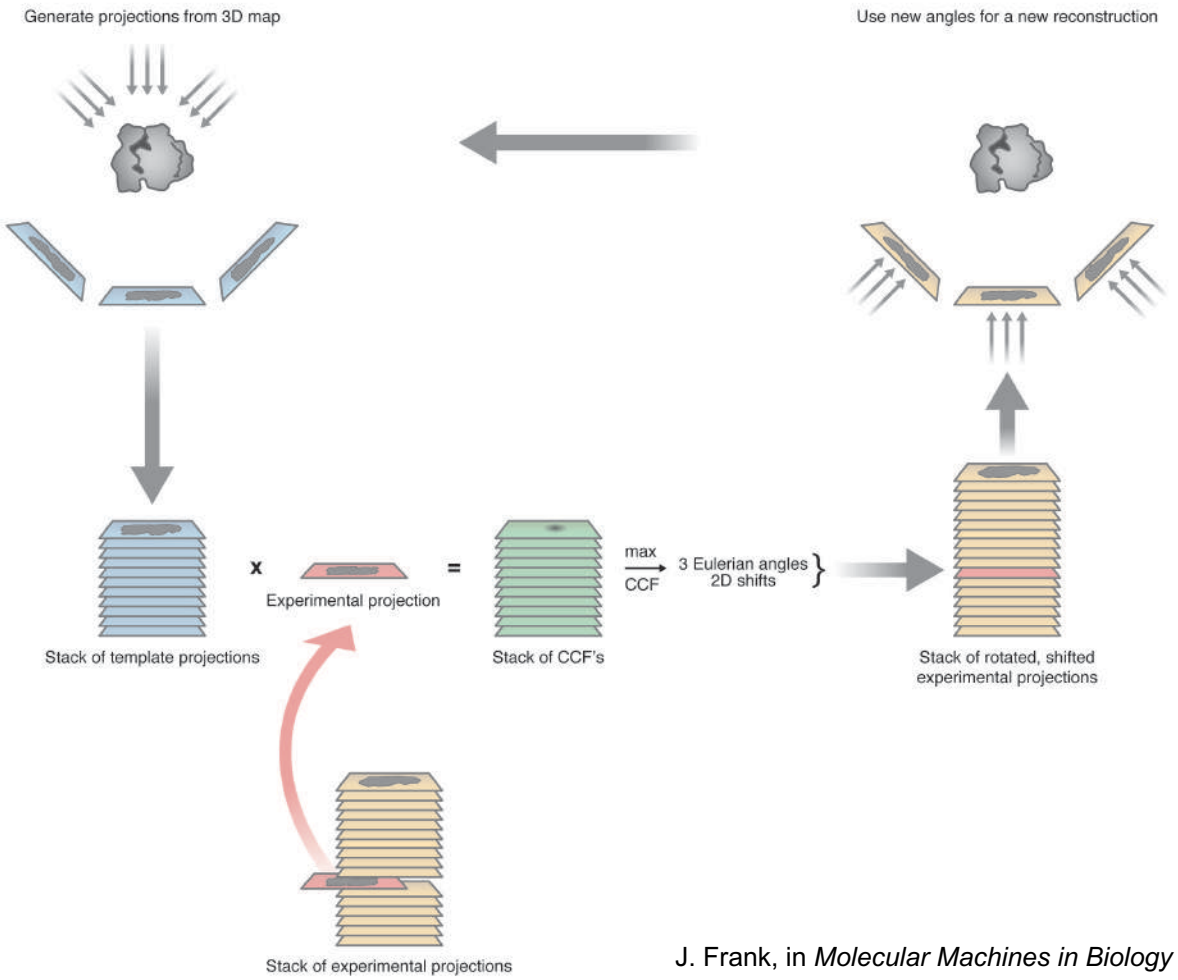

J. Frank, in *Molecular Machines in Biology* 2011

E. coli ribosome

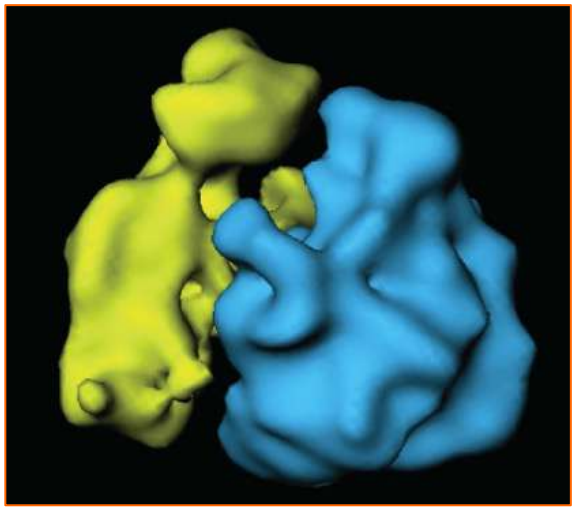

Frank et al., Nature 1995

Octopus hemocyanin

Lambert et al., 1994

Calcium Release Channel

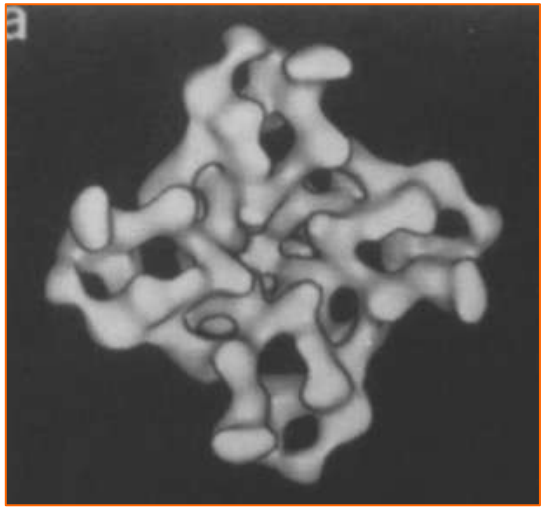

Radermacher et al., 1994

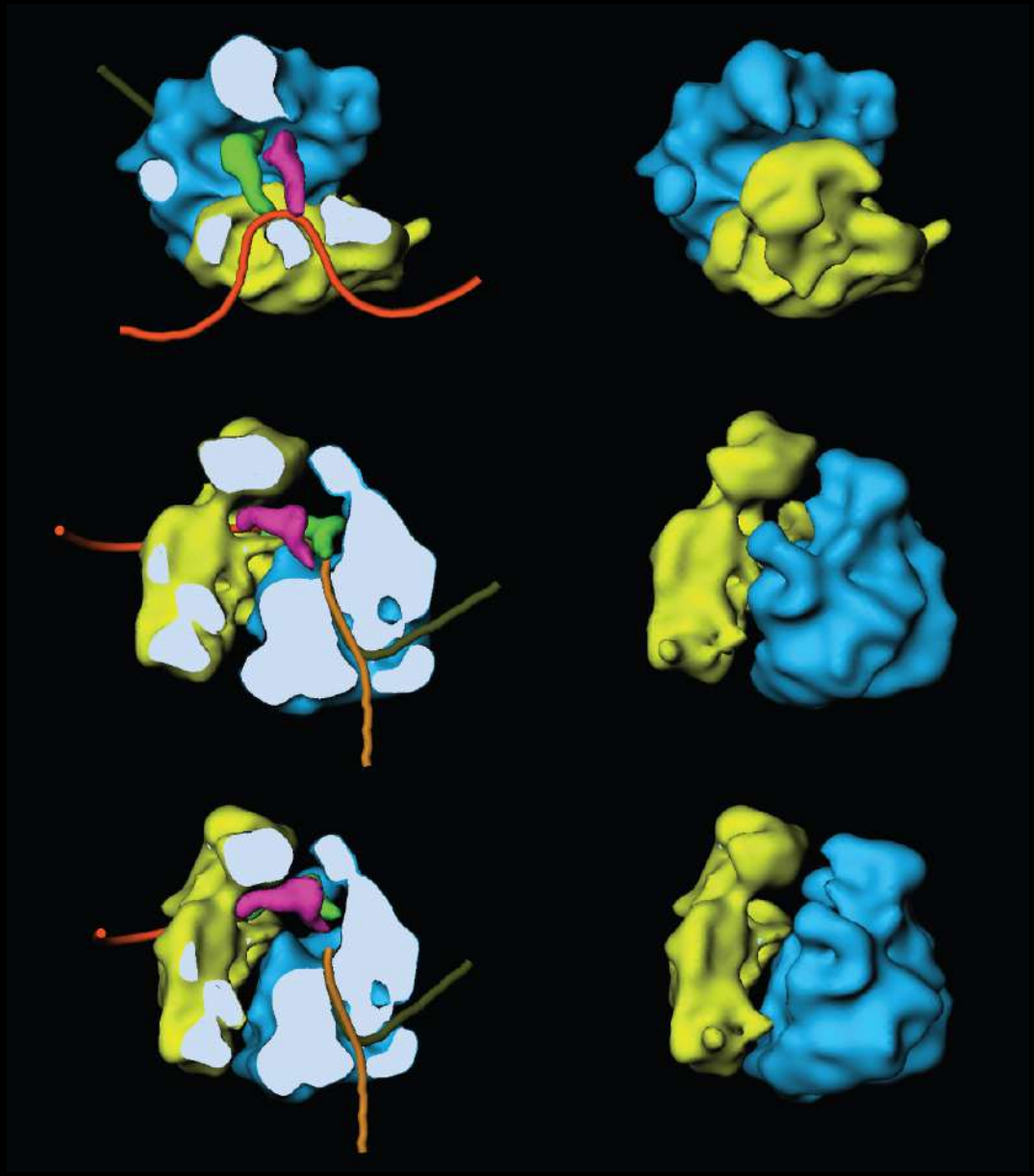

E. coli ribosome 1995

Elongation Cycle (for adding each amino acid)

Decoding

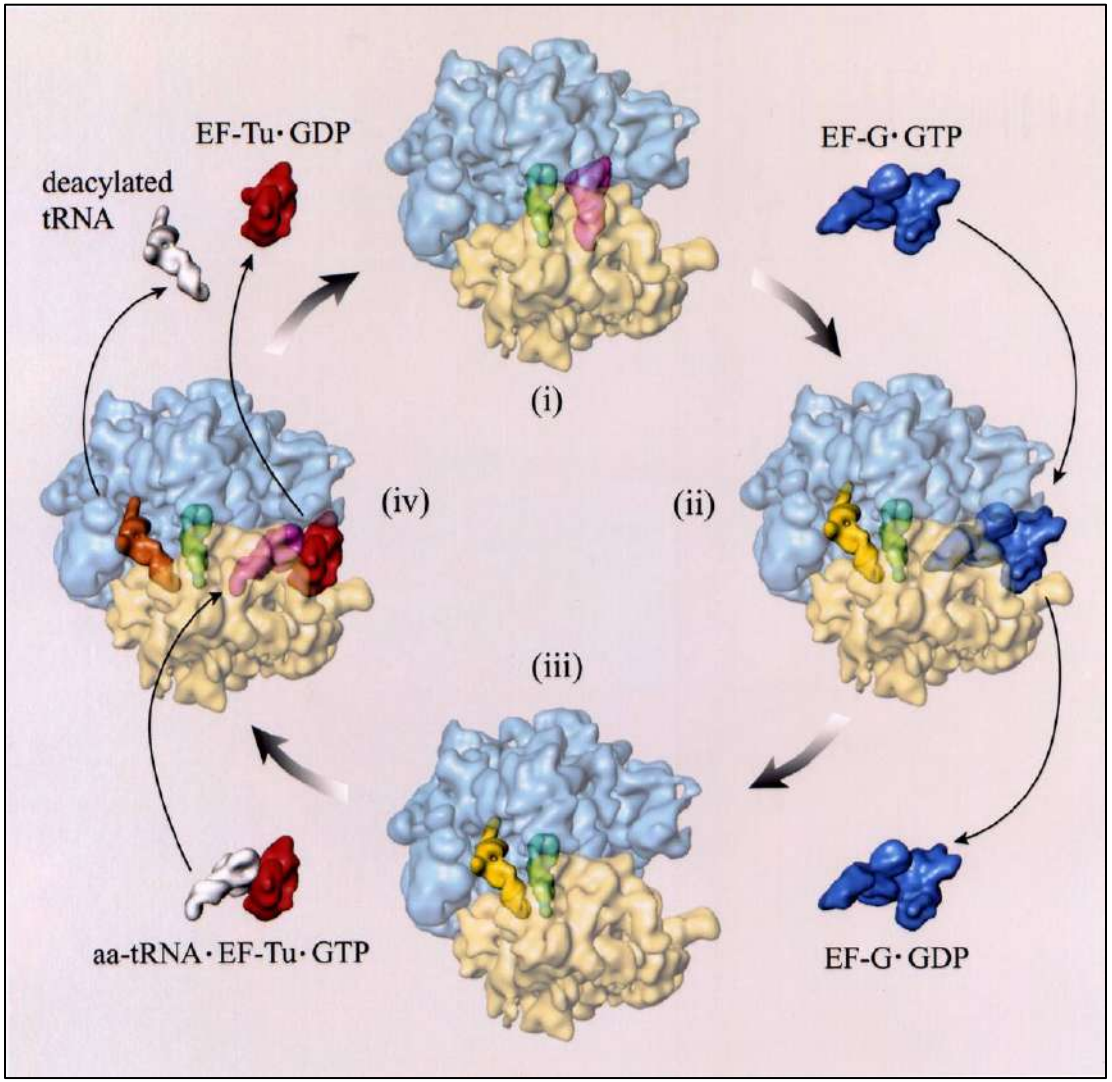

Translocation

Maximum likelihood method of classification

Several reconstructions from the same sample all at once!

"STORY IN A SAMPLE"

S.H.W. Scheres, H. Gao, M. Valle, G.T. Herman, P.P.B. Eggermont, J. Frank & J.M. Carazo (2007). "Disentangling conformational states of macromolecules in 3D-EM through likelihood optimization." *Nat. Methods*, 4, 27-29.

S.H.W. Scheres (2012). "A Bayesian View on Cryo-EM Structure." J. Mol. Biol. 415, 406-418.

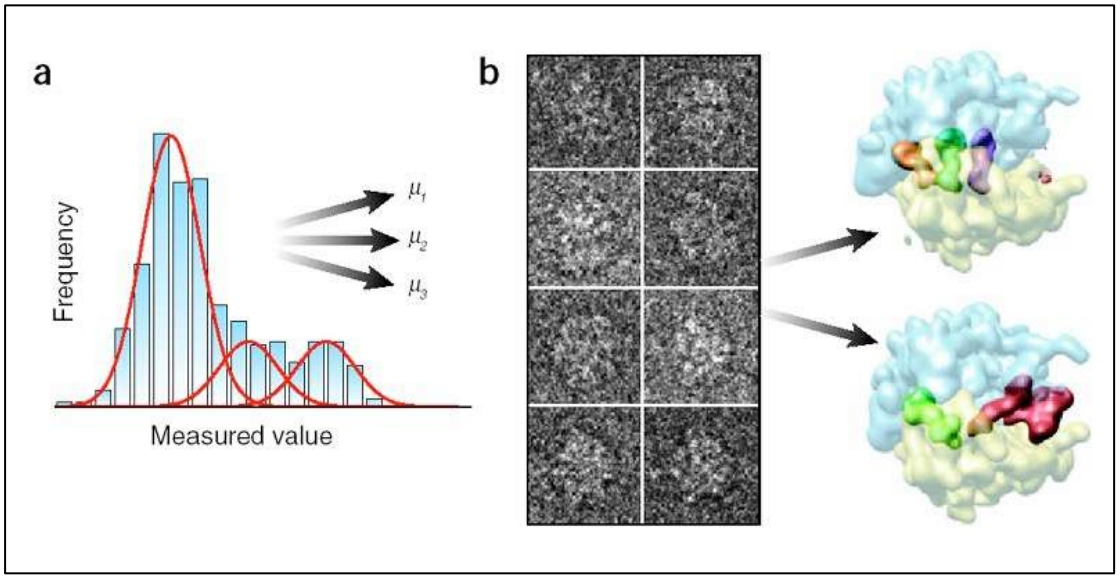

"**STORY IN A SAMPLE**" -- intermediate states in the ratchet-like motion and hybrid tRNA positions in the absence of EF-G

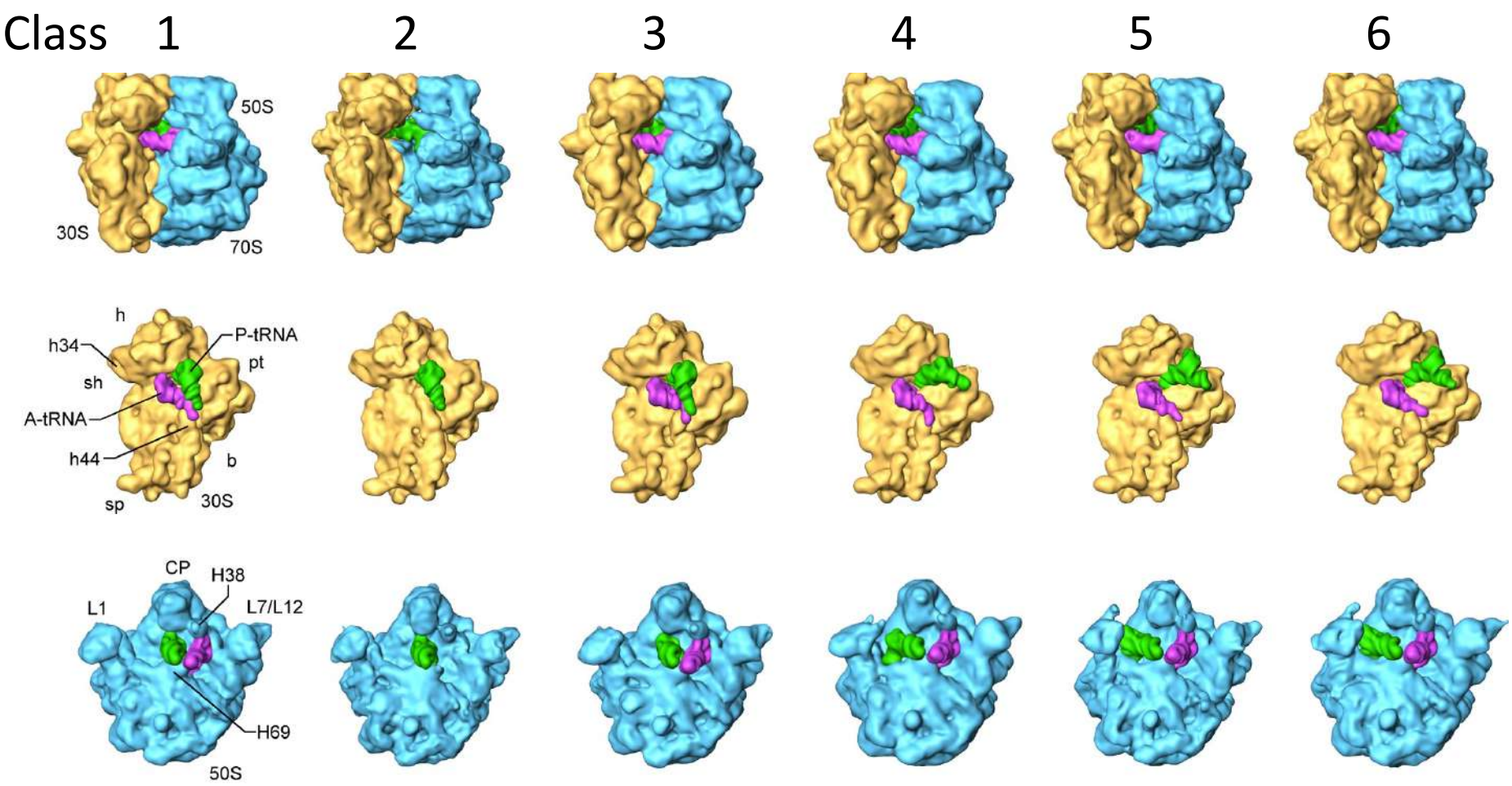

Agirrezabala et al., PNAS 2012

Resolution of single-particle cryo-EM was limited by the inferior quality of the recording medium

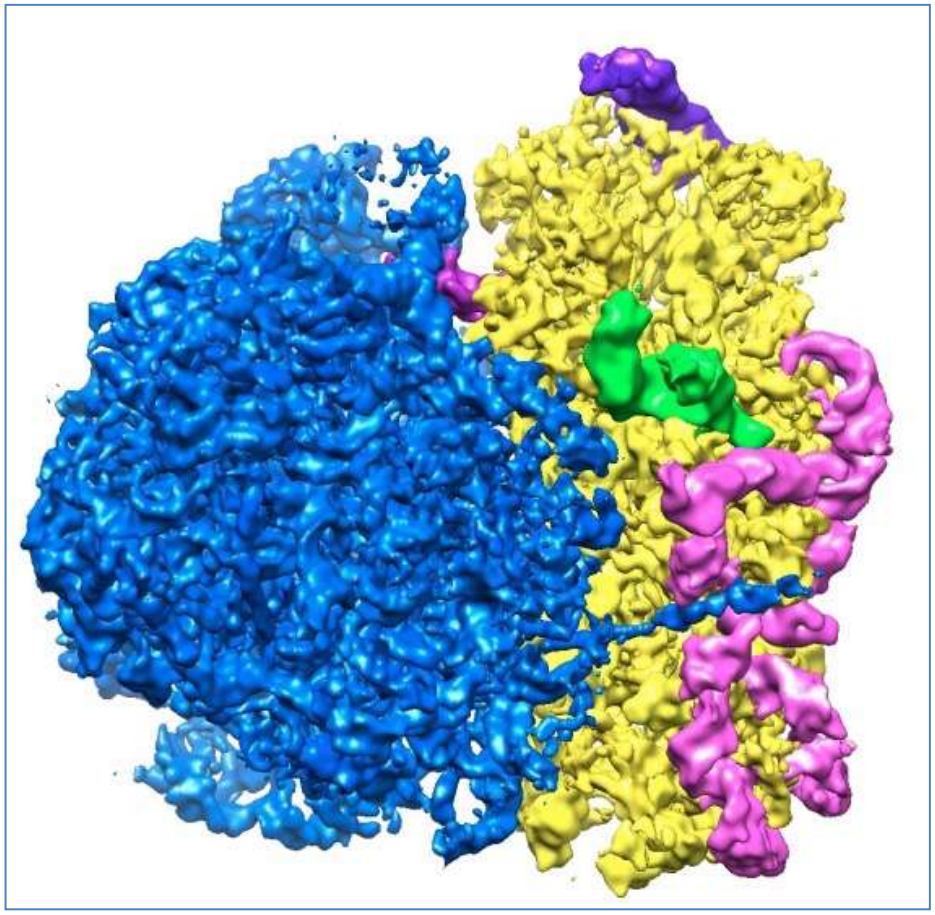

Hashem et al., Nature 2013

Best resolution from recording on film: 5.5Å

NEW ERA (SINCE 2012): DIRECT ELECTRON DETECTING CAMERAS

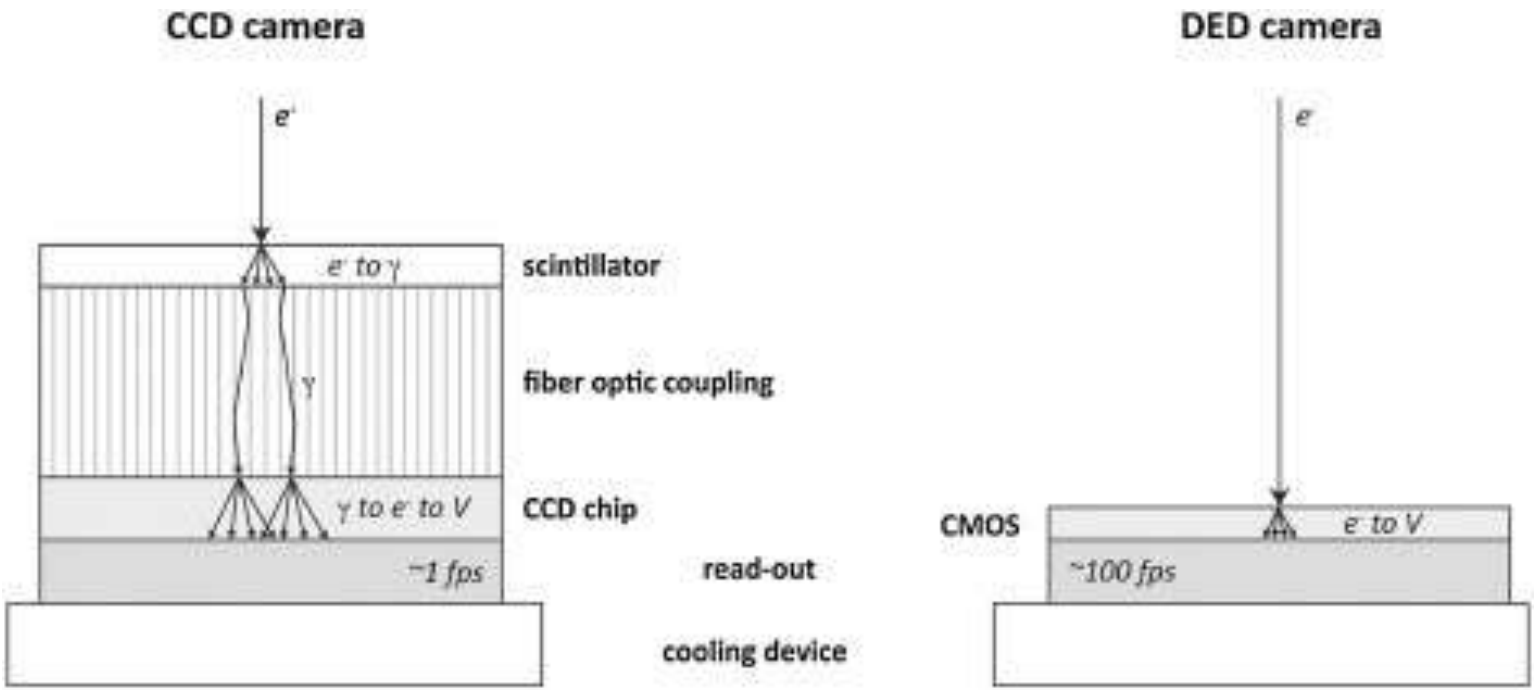

Koning et al. Ann. Anatomy 2018

New era (since 2012): *New single-electron detecting cameras*

Detection Quantum Efficiency (DQE):

(how good is the recording device in capturing every single electron?)

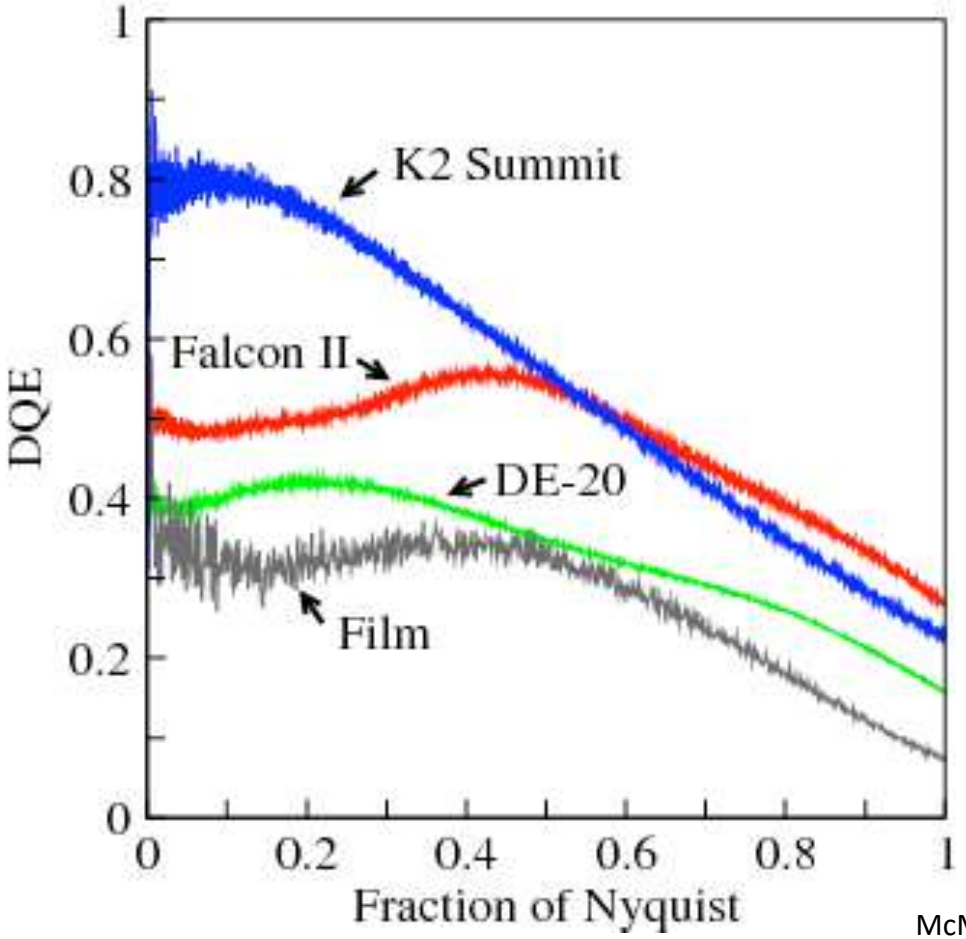

McMullan, G. et al. arXiv:1406.1389

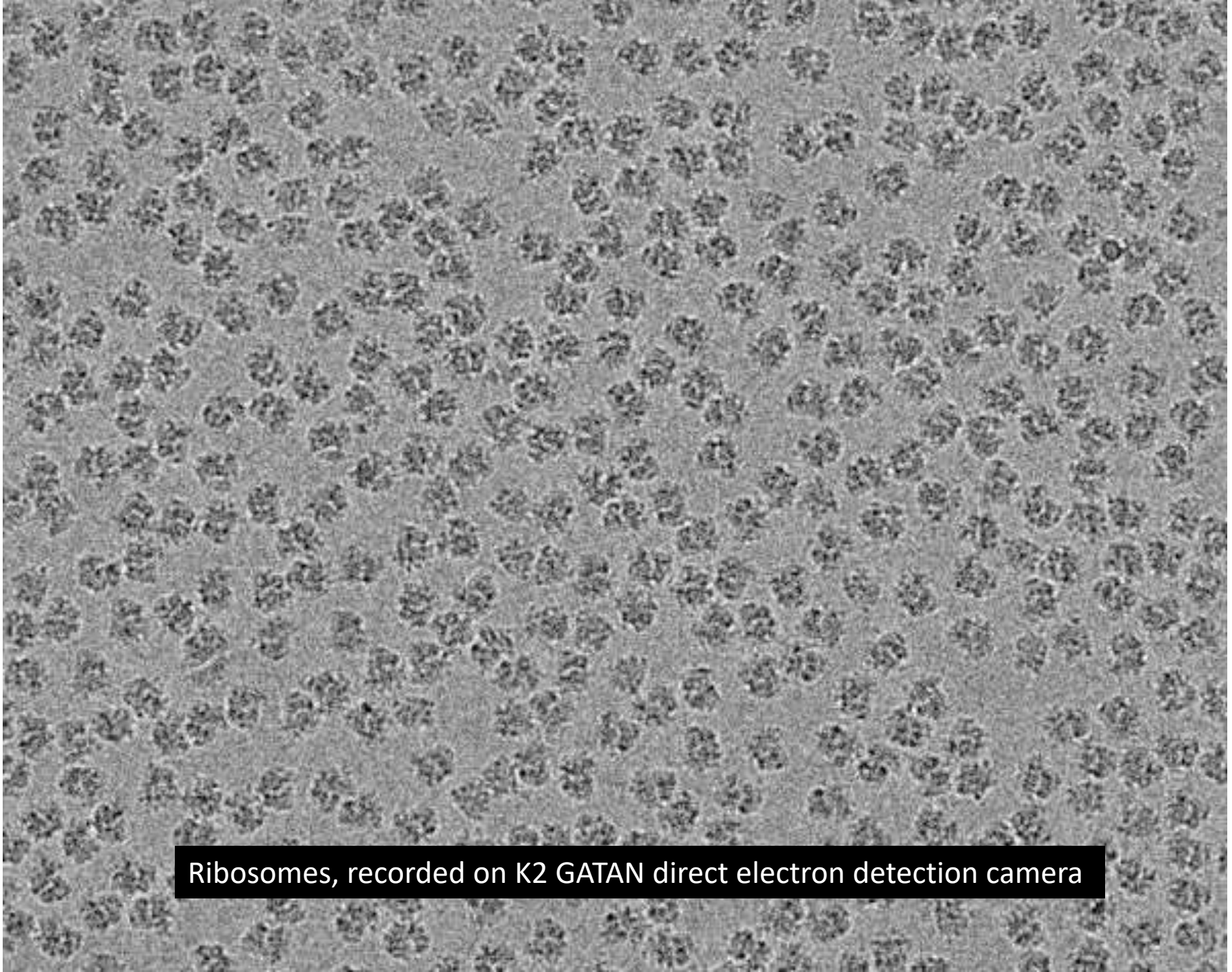
Ribosomes, recorded on K2 GATAN direct electron detection camera

WORKFLOW FROM SAMPLE TO ATOMIC STRUCTURE

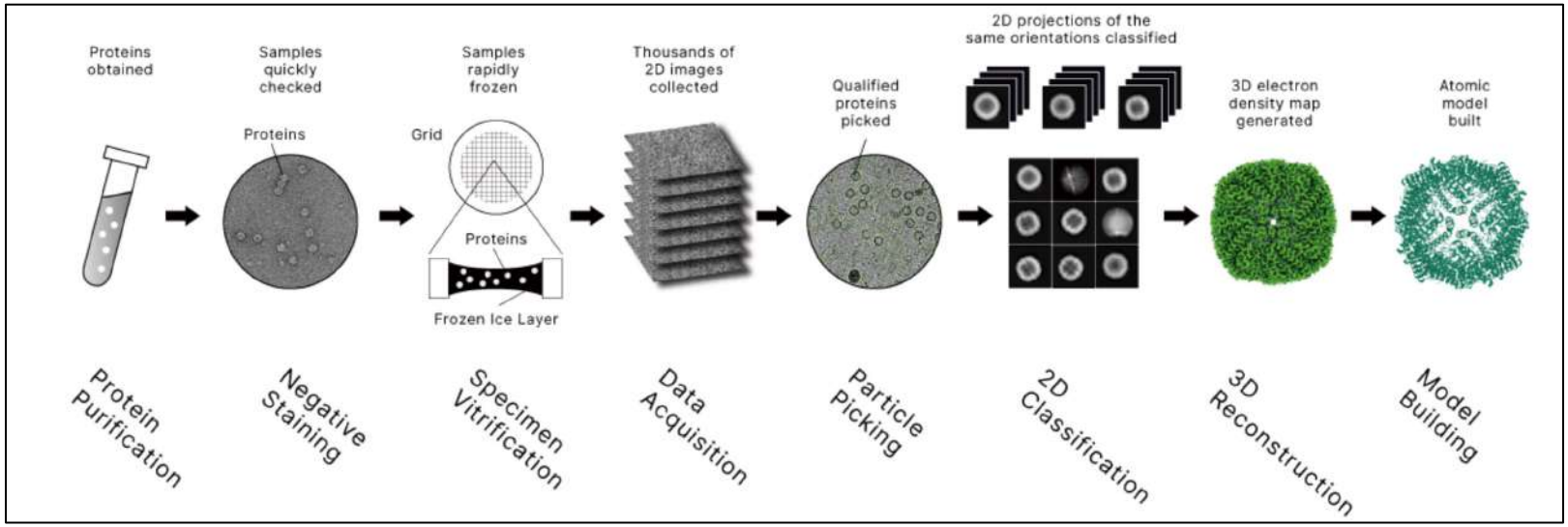

https://shuimubio.com/services/cryo-em-spa

Elongation Factor G mutant H94A bound to the ribosome

nr 70S--P-E

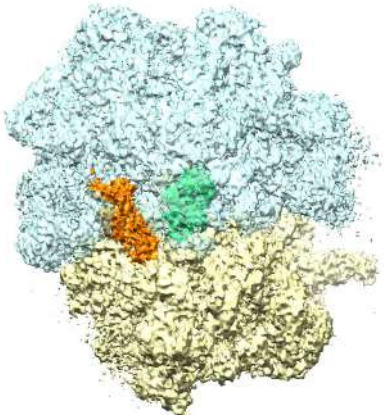

50,000

nr 70S--EF-G—P-E

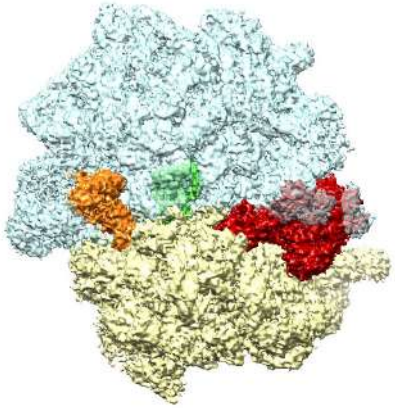

90,000

r 70S—EF-G—P/E

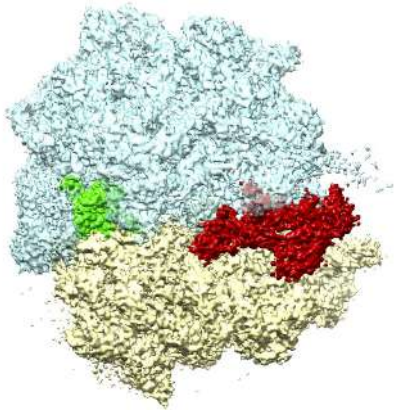

35,000

r 70S—P/E

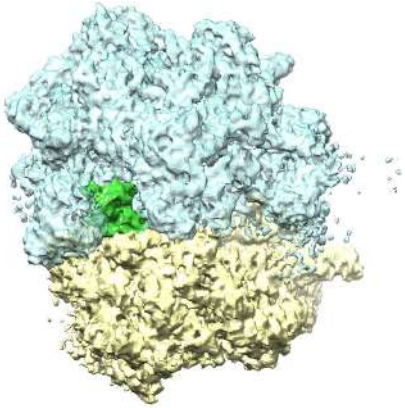

15,000

Example for maximum likelihood 3D classification
Multiple states in the same sample

Li et al., Science Advances 2015

T. cruzi ribosome large subunit at 2.5 Å

Liu et al., PNAS 2016

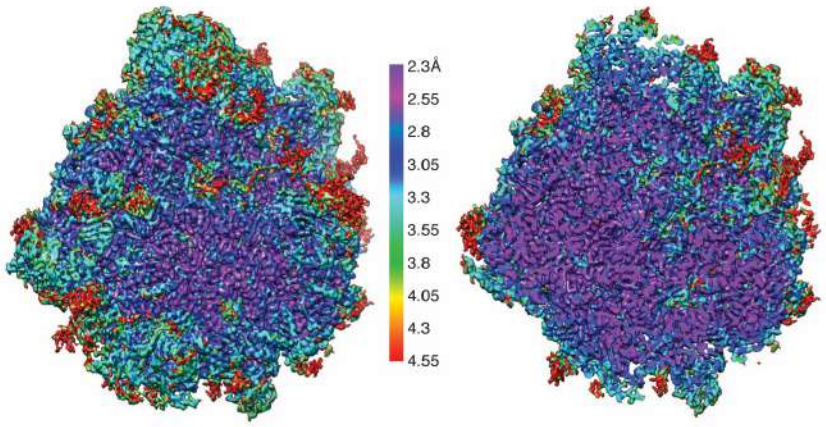

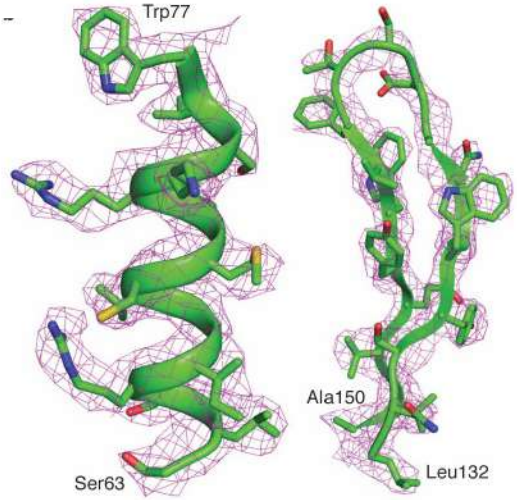

α-helix 2 strands of β-sheet

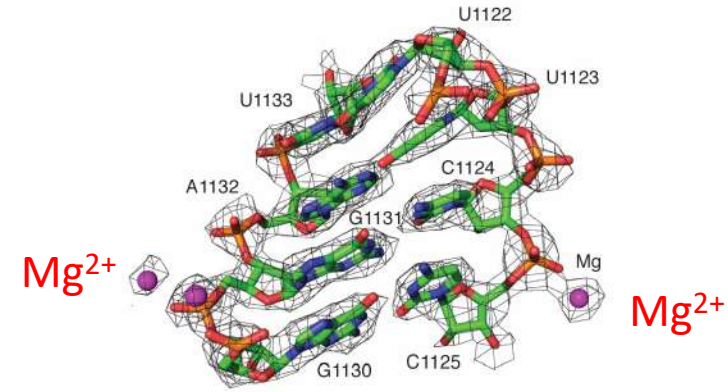

Mg^{2+} Mg^{2+}

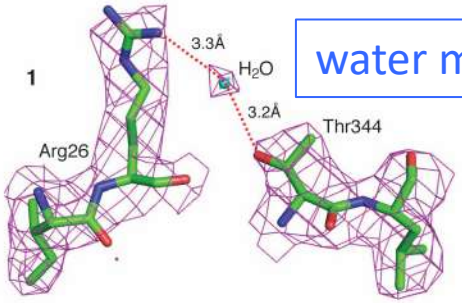

water molecule!

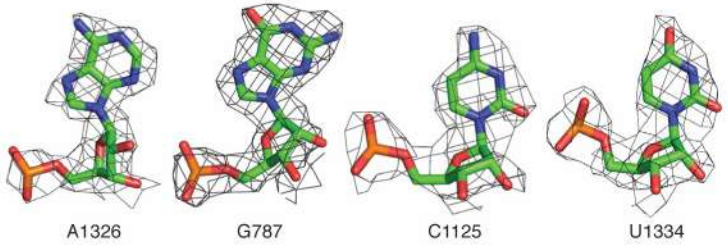

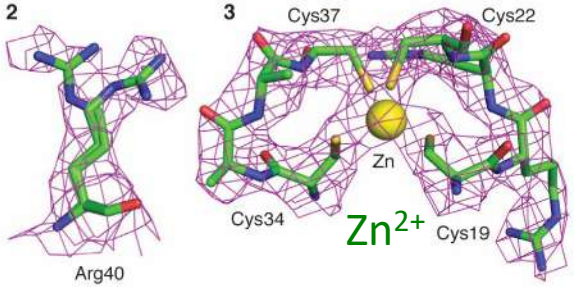

Zn^{2+}

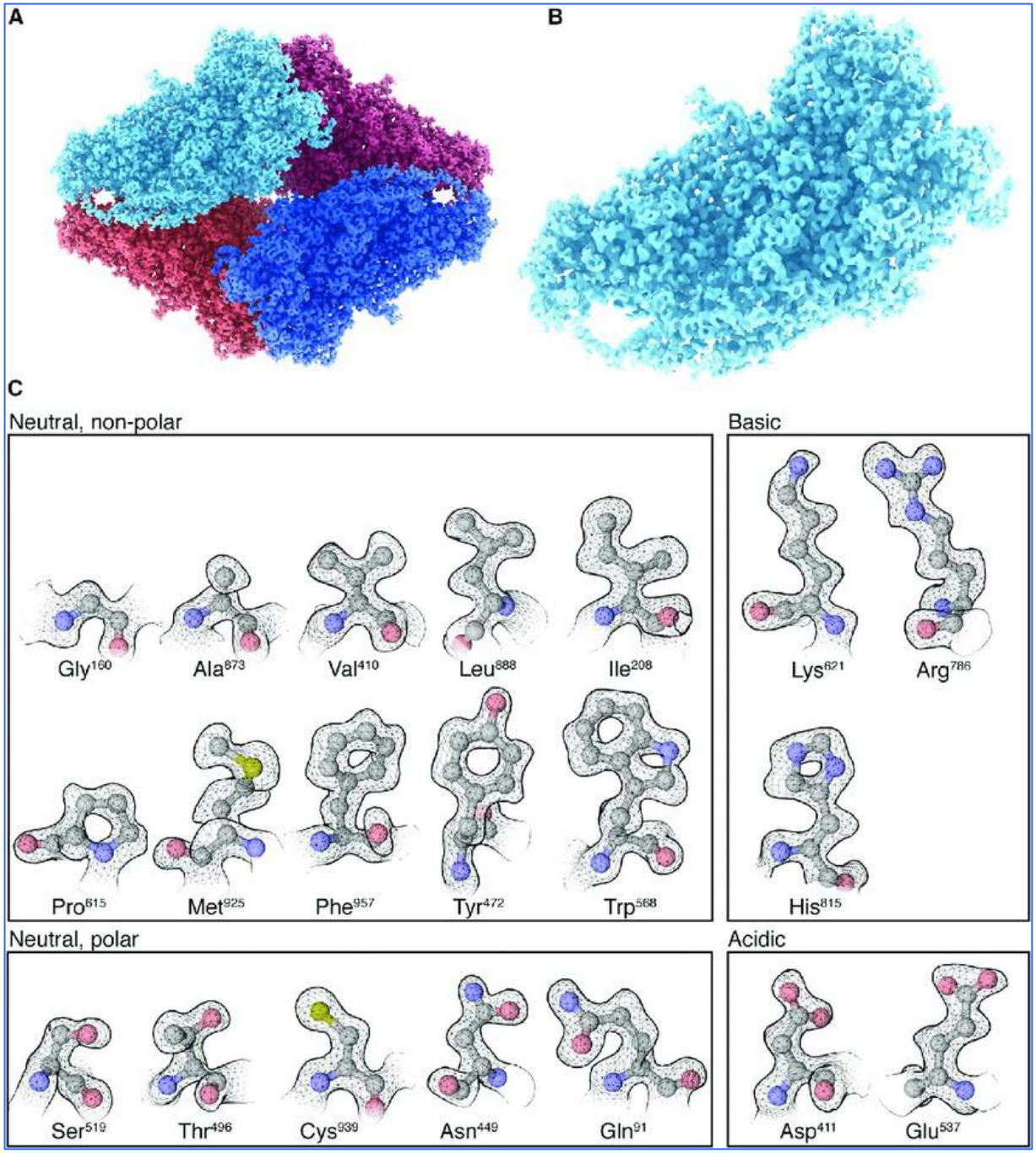

Bartesaghi et al.
STRUCTURE 2018

Beta-Galactosidase
At 2.2 Å resolution

“Signatures” of amino acids in the Coulomb density distribution

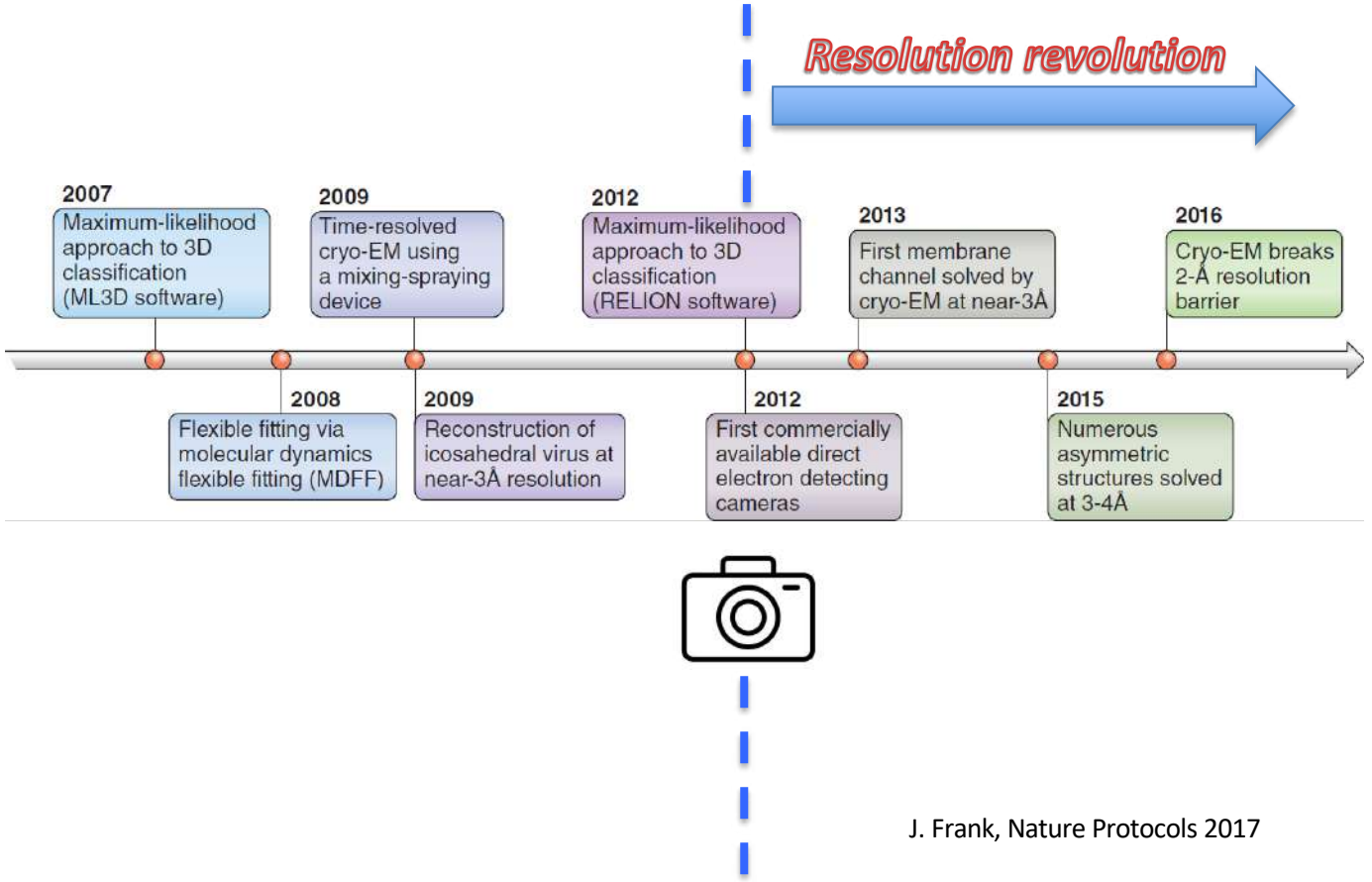

J. Frank, Nature Protocols 2017

Just in Time: high-resolution single-particle cryo-EM and the new pandemics

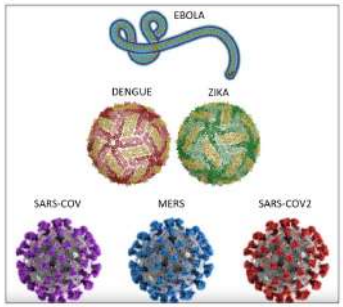

2012

2012 – 2015

MERS

2015 – 2016

Zika

Ebola

2014 – 2016

2020 - ????

SARS-Cov2

Dengue

2019 – 2020

Fig. 4: Cryo-EM reconstructions of Fab–spike complexes and visualization of neutralizing epitopes on the spike surface.

From: Potent neutralizing antibodies against multiple epitopes on SARS-CoV-2 spike

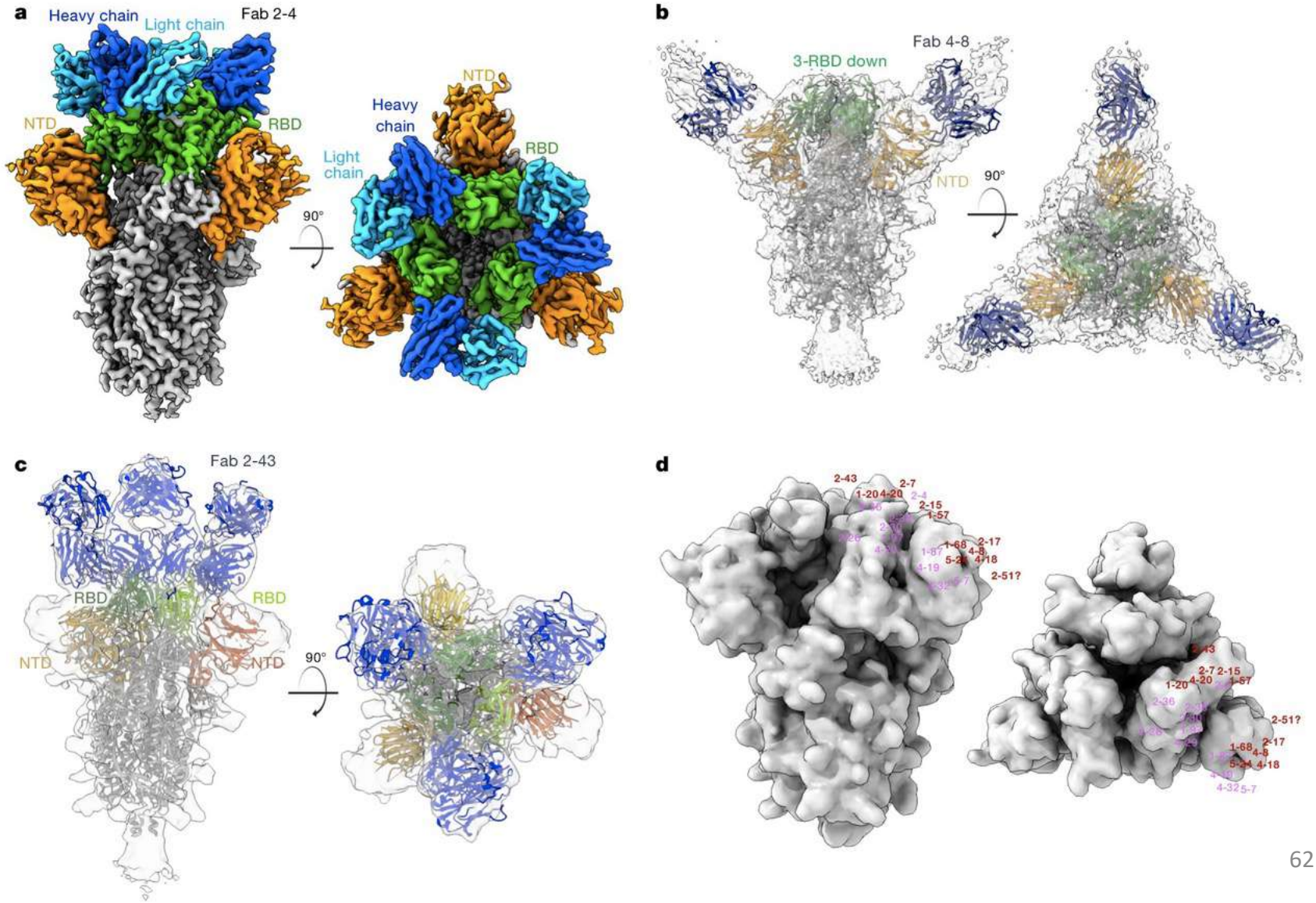

of released structures (PDB) / year

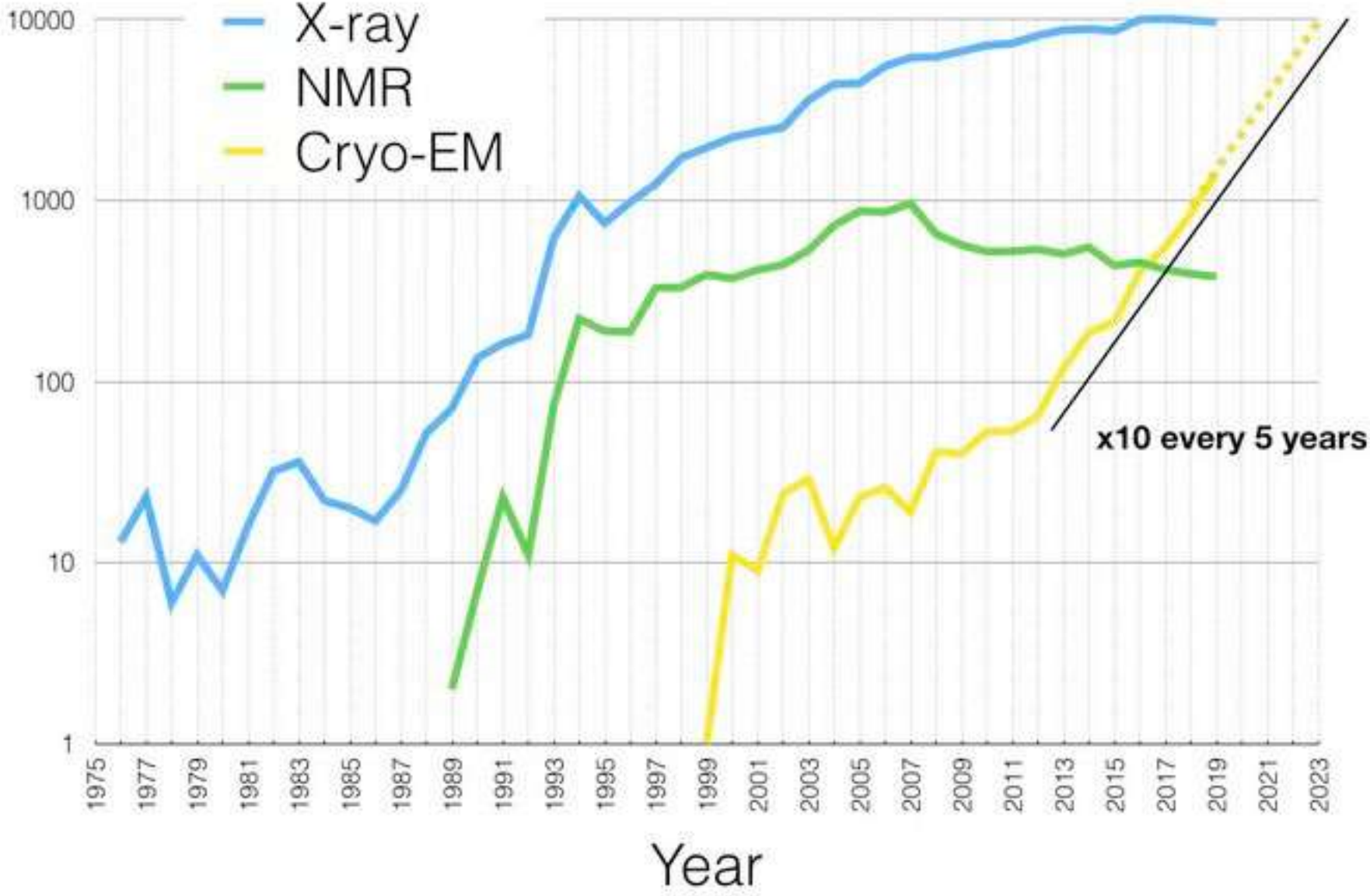

Future directions

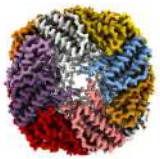

Higher spatial resolution

Time resolution
microfluidics

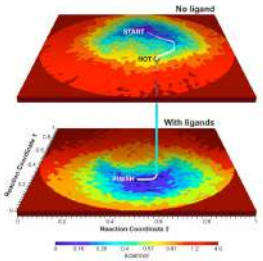

State resolution
machine learning
energy landscape

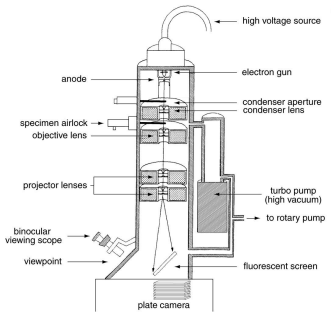

Time-resolved cryo-EM

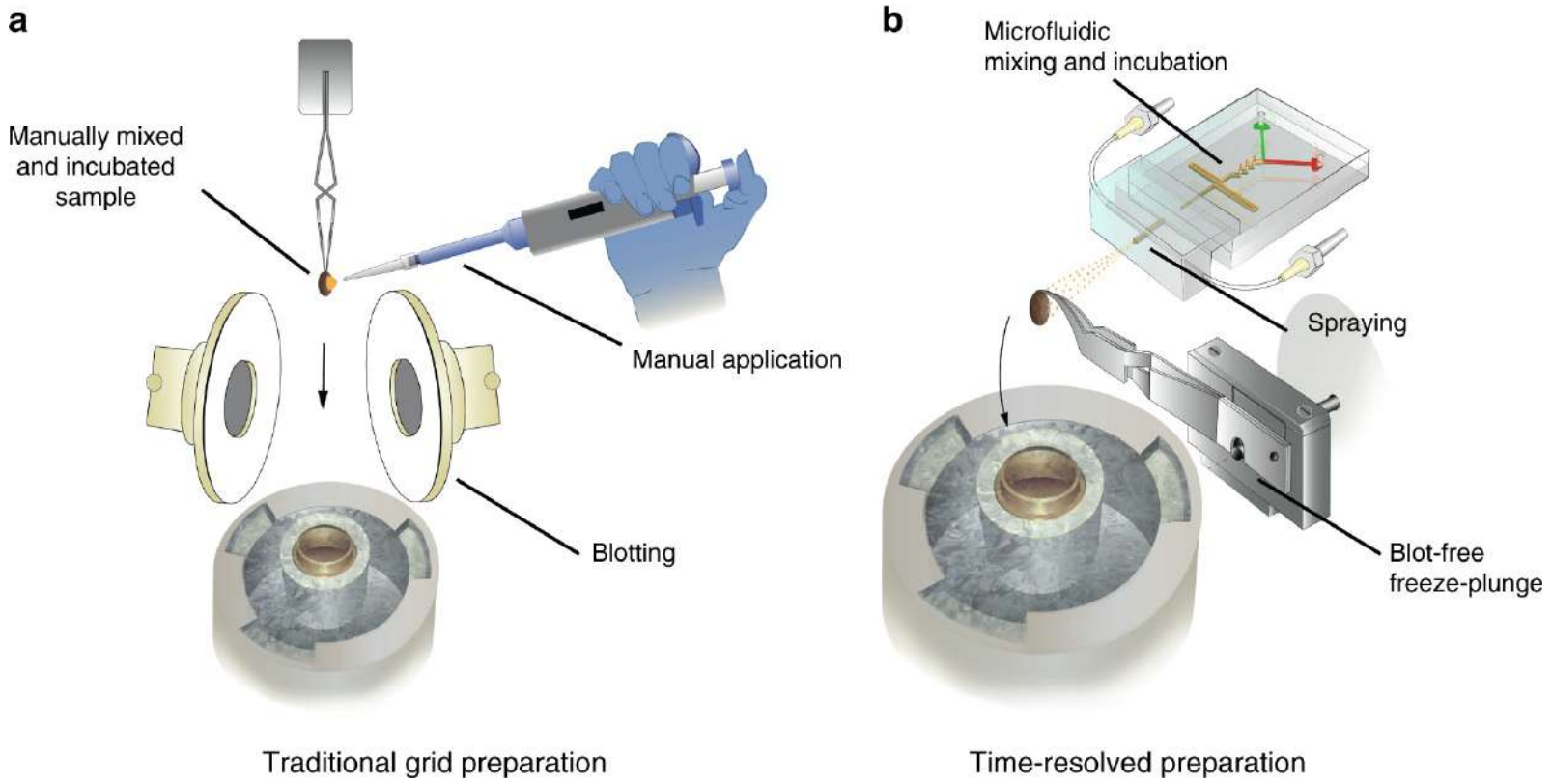

Mäeots et al. Nat. Commun. 2020

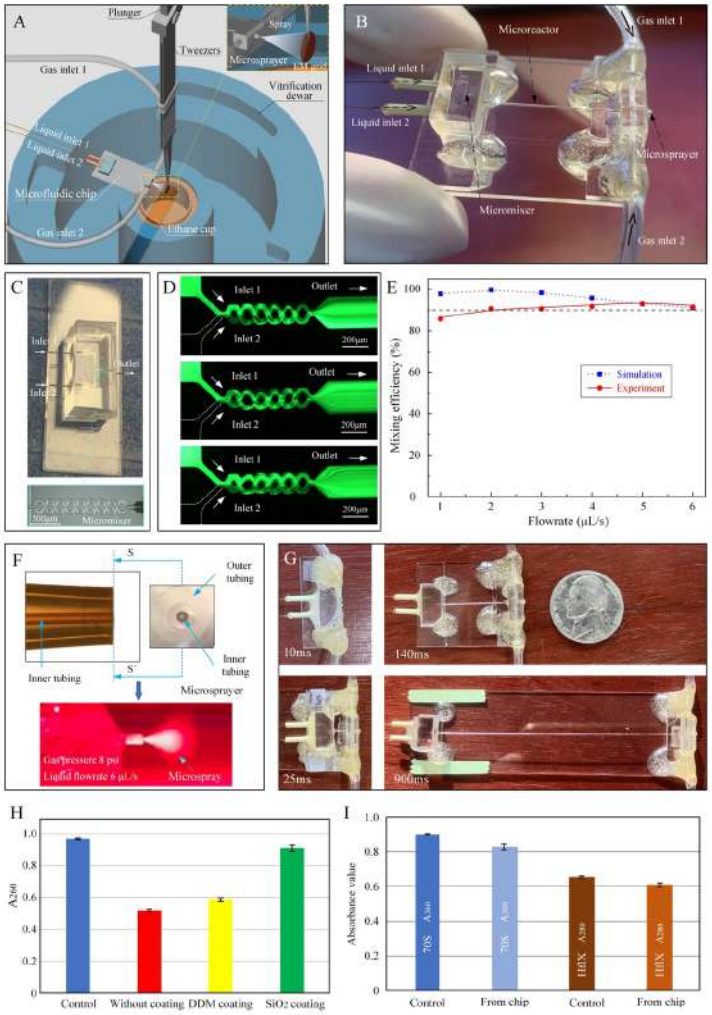

PDMS-BASED MICROFLUIDIC CHIP

Modular design

High (>90%) mixing efficiency

SO_2 coating prevents adhesion of molecules

3D sprayer

Ice thickness control

Xiangsong Feng

Bhattacharjee et al., Cell 2024

Time resolution in cryo-EM using a PDMS-based microfluidic chip assembly and its application to the study of HflX-mediated ribosome recycling

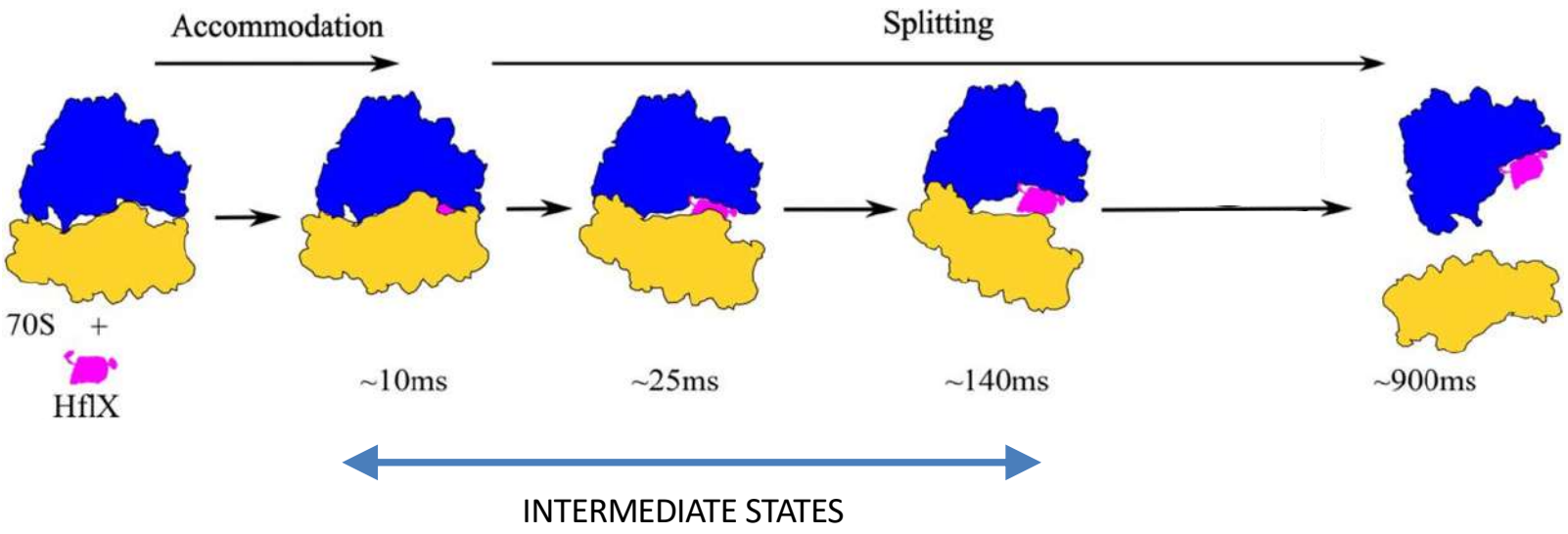

Bhattacharjee et al., Cell, in press

Literature on Time-resolved cryo-EM by Frank Lab:

Applications so far in the bacterial translation field

Shaikh et al., PNAS 2014 – ribosome subunit association

Chen et al., Structure 2015 – ribosome subunit association

Frank, J., J. Struct. Biol. 2017 -- review

Fu et al., Structure 2018 – RRF-mediated ribosome recycling

Kaledhonkar et al., Nature 2019 – translation initiation

Fu et al., Nature Comm. 2019 – translation termination

Bhattacharjee et al., Cell 2024 – PDMS-based microfluidic chip assembly and HflX-mediated ribosome recycling

Other Labs:

See literature quoted in Bhattacharjee et al., Cell 2024

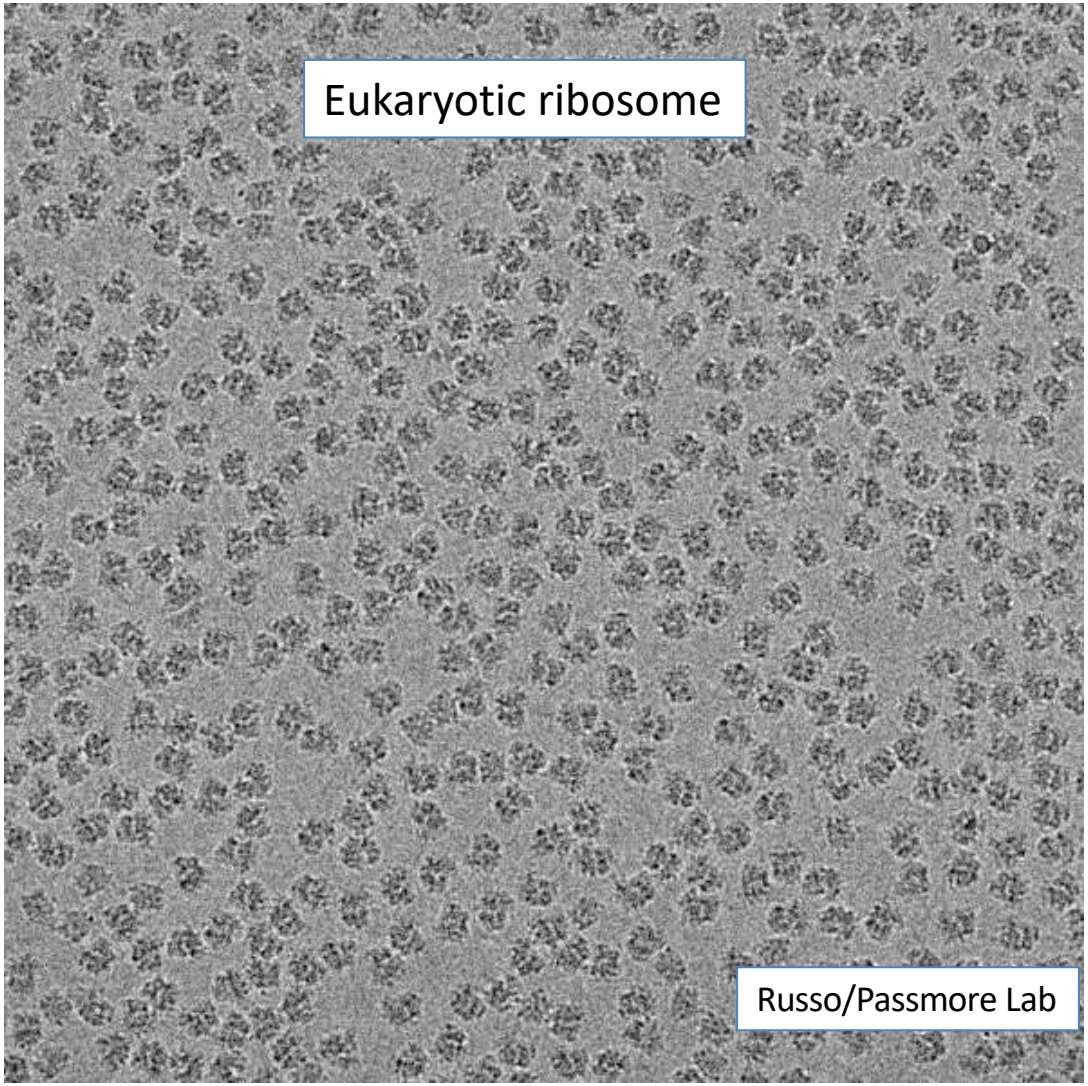
Eukaryotic ribosome
Russo/Passmore Lab


10,000 horses galloping

DO FOR EACH PD of the angular sphere:
order the images sequentially by similarity

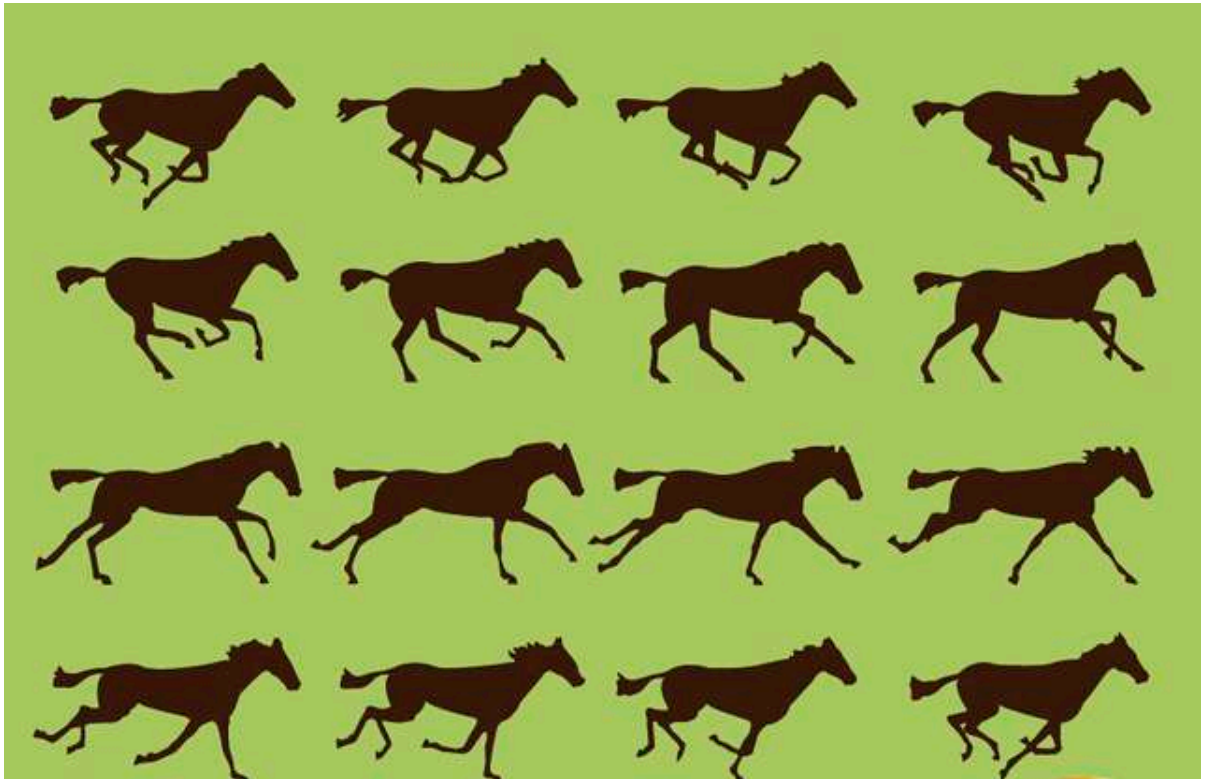

(This is a one-dimensional problem)

By splicing all images from different horses in the sequence of their similarity
in forward and backward direction, we get a movie of the average horse galloping

- Reconcile the information from all PDs (Propagation of conformational coordinates across the angular space S^2)
- Next: transform map of occupancies into free energy map.
- Low occupancy → high ΔG
- High occupancy → low ΔG

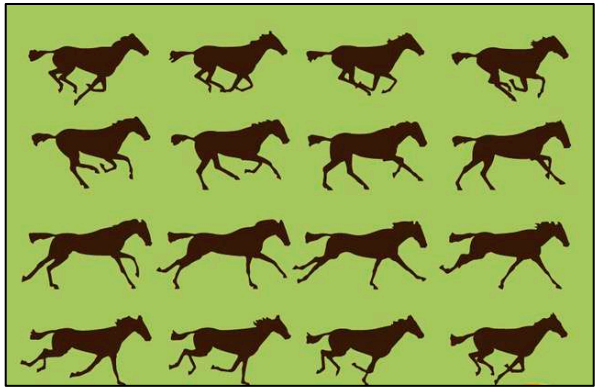

$$\Delta G / k_B T = - \ln (n_c / n_0)$$

Fischer et al. Nature 2010
Agirrezabala et al. PNAS 2015

Free energy difference | Boltzmann const. | Temperature | No. of mol. in a state | No. of mol. in most pop. state

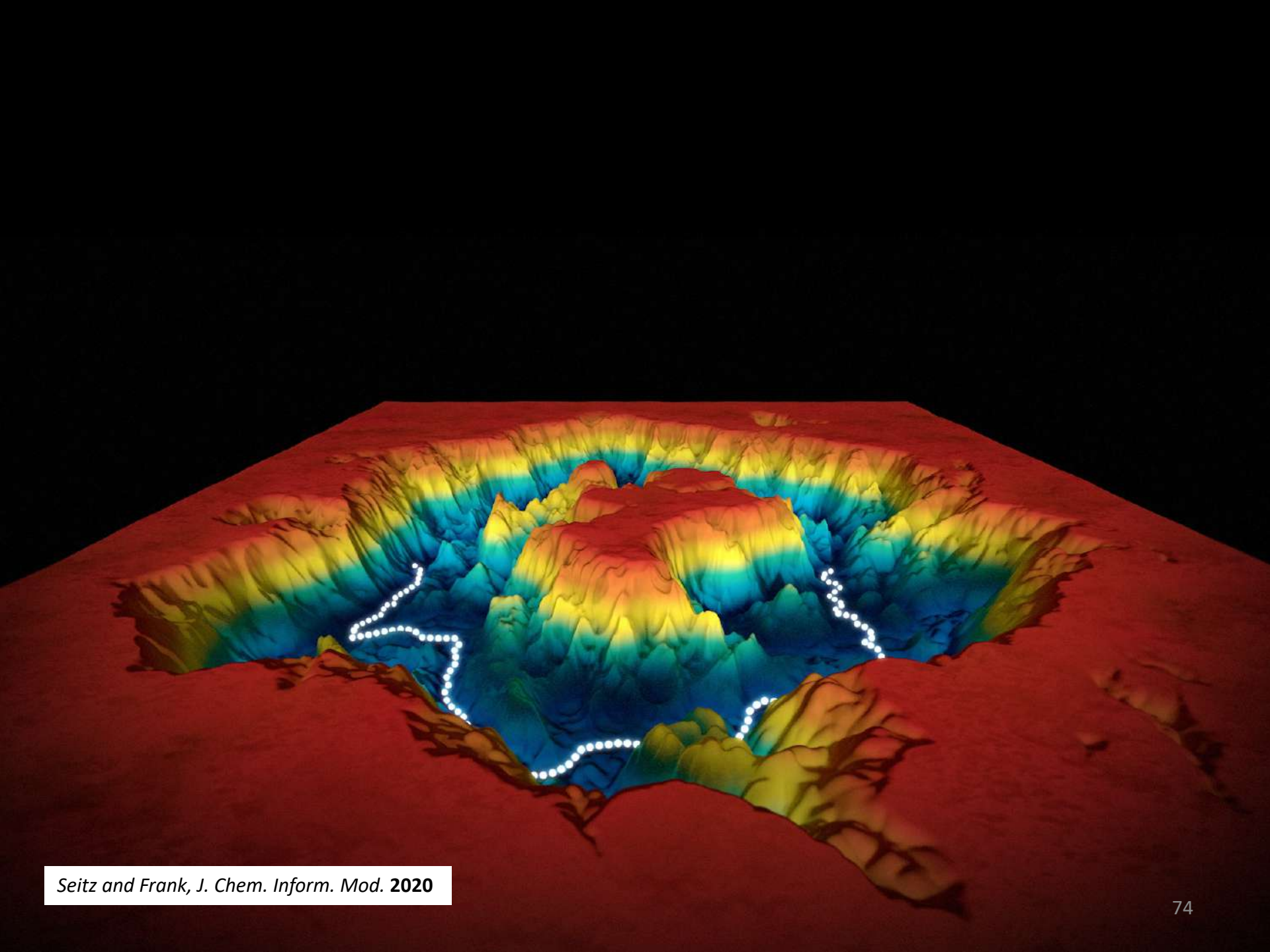

Seitz and Frank, J. Chem. Inform. Mod. **2020**

Literature on data mining from snapshots of large ensembles of molecules/ Manifold embedding/ ManifoldEM

--Dashti, A. et al. (2014). Trajectories of the ribosome as a Brownian nanomachine. *Proc Natl Acad Sci USA*

Frank, J., and Ourmazd, A. (2016) Continuous changes in structure mapped by Manifold Embedding of single-particle data in cryo-EM. *Methods* (Review)

--Ourmazd, A. (2019) Cryo-EM, XFELs and the structure conundrum in structural biology. *Nature Meth.* (Review)

--Dashti, A. et al. (2020). Retrieving functional pathways of biomolecules from single-particle snapshots. *Nature Communications*

--Seitz, E., and Frank, J. (2020) POLARIS: Path of Least Action Analysis on Energy Landscapes. *J. Chem. Inf. Model.*

--Maji, S. et al. (2020) Propagation of conformational coordinates across angular space in mapping the continuum of states from cryo-EM data by manifold embedding. *J. Chem. Inf. Model.*

--Sztain, T. et al. (2021). A glycan gate controls opening of the SARS-CoV-2 spike protein. Nature Chemistry

--Seitz, E. et al. (2022) Recovery of conformational continuum from single-particle cryo-EM images: Optimization of ManifoldEM informed by ground truth. *IEEE Trans. Comp. Im.*

--Seitz, E. et al. (2023) Beyond ManifoldEM: geometric relationships between manifold embeddings of a continuum of 3D molecular structures and their 2D projections. *Digital Discovery*

Conclusion -- Single-particle cryo-EM: A new era in structural biology

- No need for crystals!
- *Compared to X-ray cryst., very small sample quantity needed*
- Resolution in the 3-4 Å range now routinely achievable
- *Multiple structures retrieved from the same sample → clues on function*
- Molecules in close-to-native conditions
- *Solving structures of membrane proteins much easier than with X-ray crystallography*
- Huge expansion of structural data base relevant for Molecular Medicine